8. Steam generators

The art in the steam generator design is by having specified primary fluid temperature, pressure and mass flow to design a vapor production with the lowest possible content on droplets at highest possible pressure and mass flow. On this way technical discoveries like introduction of economizers, redirection of separated water into the natural circulation loop using appropriate low pressure loss high efficiency separators etc. are inevitable.

8.1 Introduction

The heat produced in a nuclear reactor core can be used in different ways:

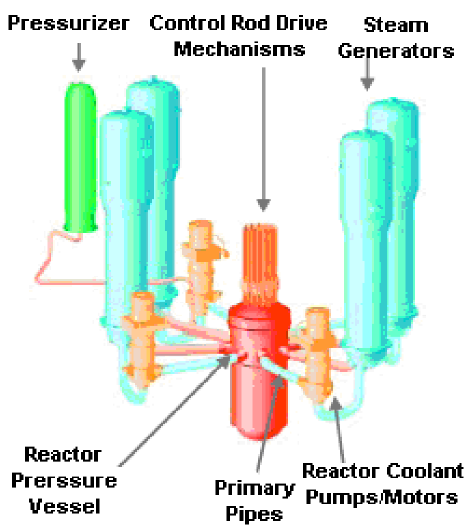

Fig. 8.1 a) European Nuclear Reactor; b) Reactor pressure vessel connected by primary pipes to the four steam generators. The four main circulation pipes and the pressurizer are visible

Boiling water reactors produce steam directly in the pressure vessel. The steam is then directed to turbines for producing mechanical work which then is transferred partially in electricity. In accordance with the Carnot's low the higher

the upper turbine entrance temperature is, the better the efficiency of the thermal cycle. In producing saturated steam the pressure is controlling the steam temperature. That is why the highest technically possible pressure is used. Recently operation at super critical pressures is intensively in investigation for this purpose – Pioro und Duffey (2007). Actually the super-critical technology is common in the conventional steam production.

The pressurized water reactors produce steam in steam generators and direct it to the steam turbines for farther use, see Fig. 8.1.

The coolant is pumped from the reactor coolant pump, through the nuclear reactor core, and through the tube side of the steam generators before returning to the pump. This cycle is called primary loop. The primary loop water with about 600 K and 150 bar flowing through the steam generator boils other water on the shell side and produce steam in the secondary loop that is delivered to the turbines to make electricity. The steam is subsequently condensed via cooled water from the tertiary loop and returned to the steam generator to be heated once again. The tertiary cooling water may be transported to cooling towers where it release large amount of heat into the environment before returning to condense more steam. Once through tertiary cooling may otherwise be provided by rivers, lakes, sees and oceans. This primary, secondary, tertiary cooling scheme is the most common way to extract usable energy from a controlled nuclear reaction. These three loops also have an important safety role because they constitute one of the primary barriers between the radioactive and non-radioactive sides of the plant as the primary coolant becomes radioactive from its exposure to the core. For this reason, the integrity of the tubes is essential in minimizing the leakage of water between the primary and the secondary sites of the plant.

8.2 Some popular designs of steam generators

8.2.1 U-tube type

Figure 8.2 is a schematic diagram of a U-tube type vertical steam generator design.

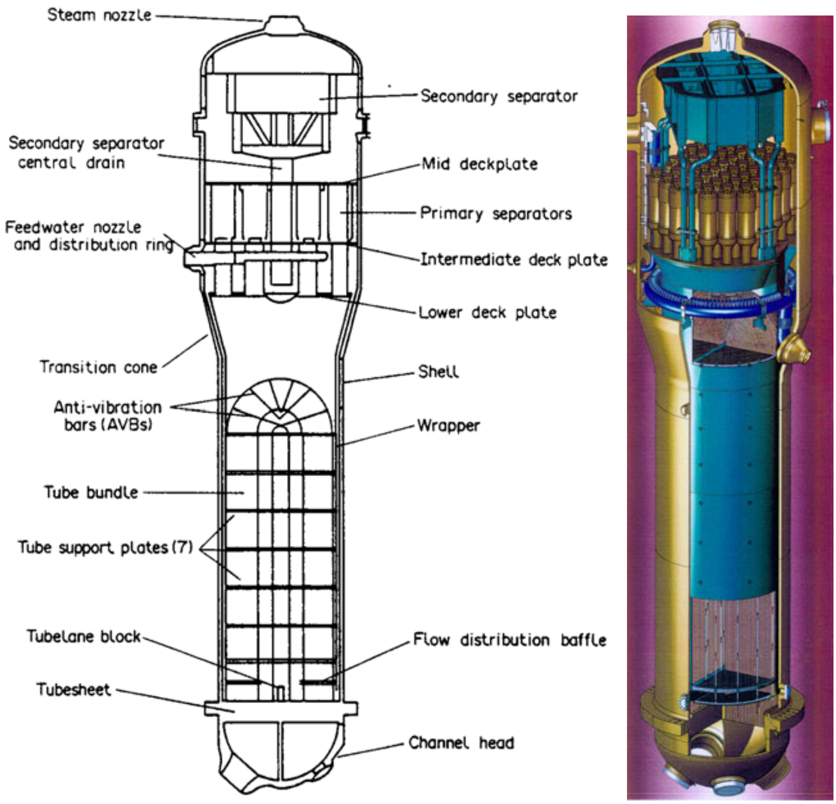

Fig. 8.2 U-tube type steam generators for nuclear power plant: a) Westinghouse Model-F design, *Singhal* and *Srikantiah* (1991); b) Siemens design, Bouecke (2000)

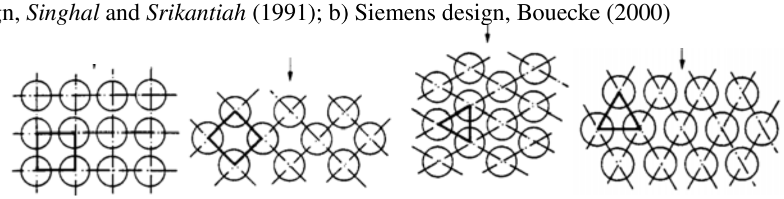

Fig. 8.3 Pipe arrangements: quadratic: (**a**) inline; (**b**) staggered; triangle: (**c**) inline; (**d**) staggered. Typically pipes with about 19–25 mm outside diameter and pich 25–37.5 mm are used, Singhal and Srikantiah (1991)

The steam generator components are contained within a cy1indrical vessel.

The primary water enters the inlet plenum of the seam generator at a pressure of about 150 bar, flows inside the U-tubes and transfers heat to the water on the shell side. It enters the steam generator at about 310-327°C and leaves at about 257-288°C. At the primary inlet, the temperature difference across the tube wall is about 36-50°C corresponding to a heat flux of 315-442 kW/m². At the primary

outlet or cold side, the temperature difference between the primary and secondary sides is about 11-14°C corresponding to a heat flux of about 94 kW/m², Green and Hetstroni (1995).

The feed water is provided at the top in the modern SGs. This feed mixes with the water returned by the steam separator and flows down in the annular space between shell and shroud called down-comer. Subsequently, this water flows upwards over the U-tubes inside the shroud, pick up heat and generates the steam. This two phase mixture rises then to steam separators. The thermodynamic quality of the water-steam mixture at the top of the bundle is about 17-33% when it enters the steam separators, which corresponds to a circulation ratio in the range of 6:1 to 3:1, Green and Hetstroni (1995). As the load decreases, the circulation ratio increases. The pressure on the secondary side is about 40 to 7.5 MPa.

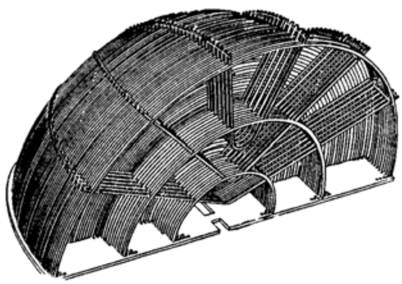

Fig. 8.4 Antivibration bar arrangement, Singhal and Srikantiah (1991)

The tubes may have quadratic or triangular arrangements each of them may be inline or staggered as shown in Fig. 8.3. In commercial power plants steam generators can measure up to 22 m in height and weigh as much as 800 tons. Each steam generator can contain 3000–16 000 tubes, each about 19 mm in diameter. In Kraftwerk Union (KWU) and later B&W/AECL designs (Babcock & Wilcox/Atomic Energy of Canada Limited), the tubes have been made of alloy 800. The mill-annealing conditions vary among the manufacturers, while B&W/AECL have used stress-relieved (680°C/8 h) tubing for their alloy 600 tubed steam generators. Some of the more recent designs using alloy 600 tubing have thermally treated tubing (704°C/11.5h) to improve resistance to stress corrosion cracking. Later designs and recent replacement units use Inconel 690 almost exclusively, Green and Hetstroni (1995). The very long tubes are exposed on flow induced oscillations and will vibrate touch each other or touch structures and erode if anti vibration spacers are not used. An example for tube support planes is given on Fig. 8.1 and for anti vibration bars in Figs. 8.2 and 8.4. Type 347-stainless-steel has always been used for KWU steam generator tube support structures.

Other design of U-tube steam separator is given in Fig. 8.5.

In all cases a primary inlet and outlets are designed as a chambers in which mixing happens. The tubes are welded on the thick tube sheet. Several redistribution plates or other design feature improve the performance of the steam generator. The upper part of the shell has larger diameter because the two phase mixture expands in this region up to the lower deck plate. The pressure retaining parts are essentially made from ASME 106 Thermal Hydraulic Design of Components for Steam Generation Plants SA 533 (plates) and SA 508 (forged nozzles). No cladding is foreseen on the surfaces. Some manufacturers provide forged courses in lieu of formed plates.

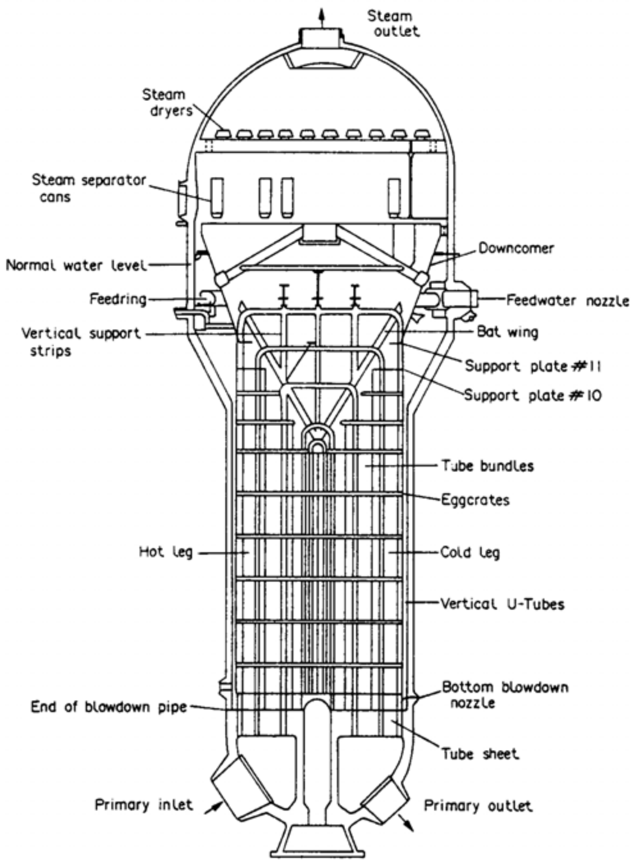

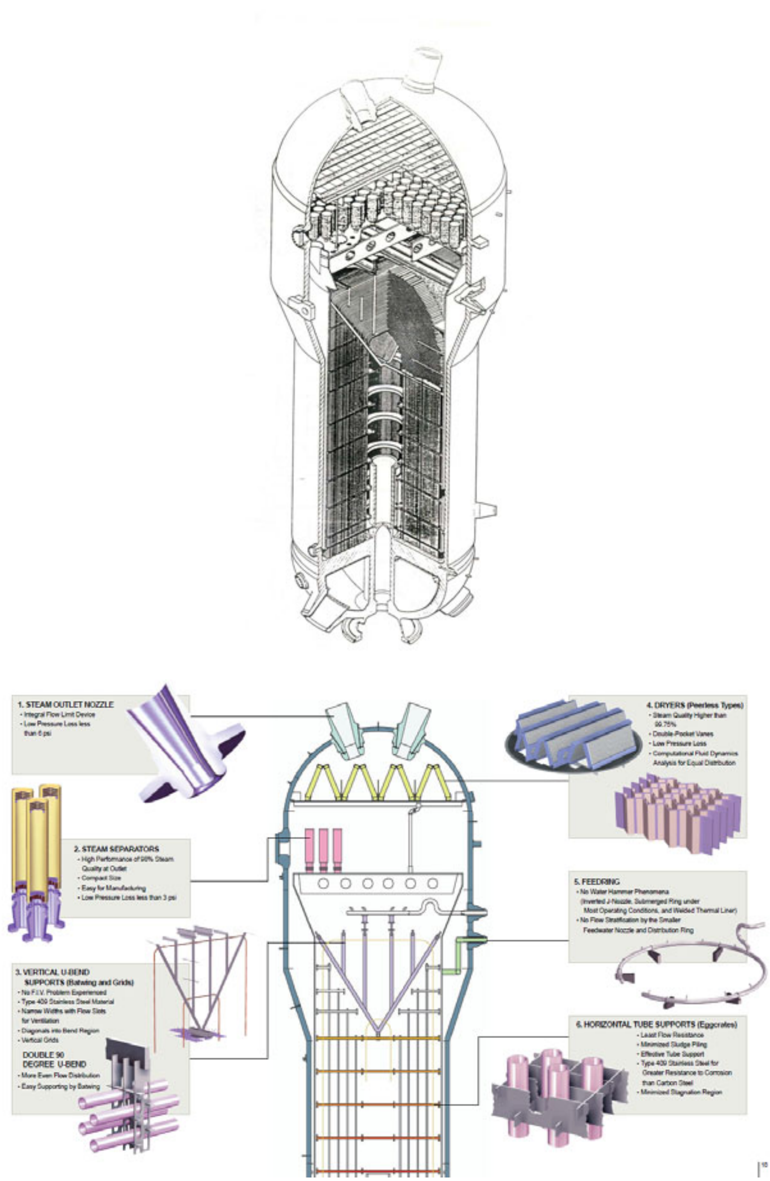

Fig. 8.5 U-tube steam generators with block separators and dryers: Combustion Engineering System-67 and System-80 design, Singhal and Srikantiah (1991), Doosan (2009a). Primary side parameter: design temperature 343.3°C, design pressure 174.7 kg/cm² abs, inlet temperature 327.3°C, outlet temperature 295.8°C, flow rate, each 27.56 x 10^6 kg/h, pressure drop 2.896bar; Secondary side parameter: design temperature 301.6°C, design pressure 87.56bar, feed-water temperature 232.2°C, Total steam flow 5.769 x 10^6 kg/h, steam pressure at 100% power 73.774bar, steam quality 99.75 %; Common parameter: primary/secondary differential pressure 155.13bar, Heat transfer rate per SG, 1414MW

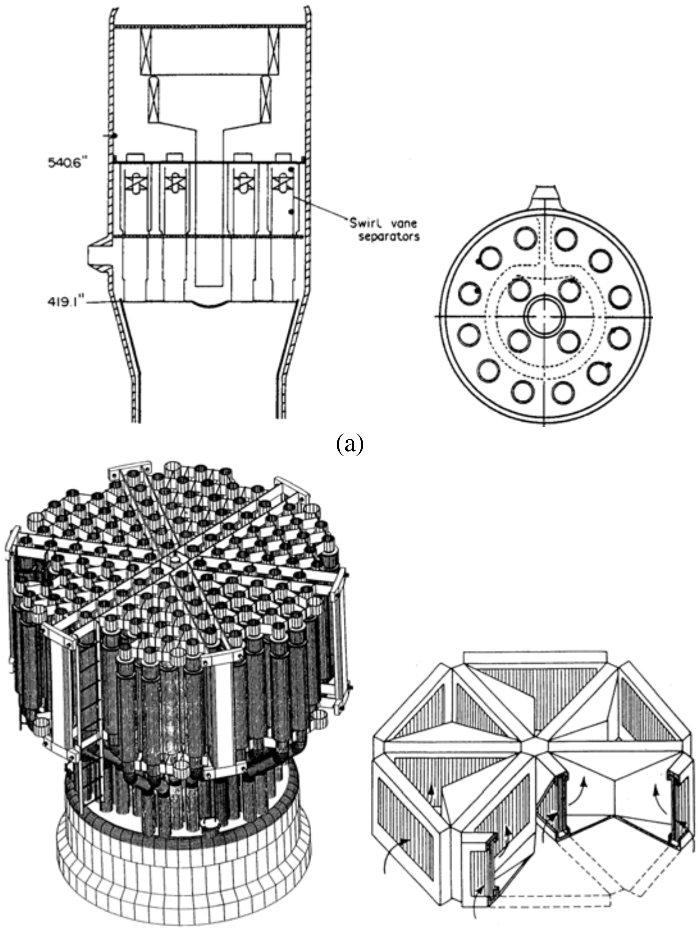

(a)

(b)

Fig. 8.6 Block of primary cyclone separators mounted on the lower deck plate; (**a**) view number large diameter cyclones, Singhal and Srikantiah (1991); (**b**) large number small diameter cyclones, Bussy et al. (1998)

As already mentioned the steam quality, i.e., the ratio of the mass of steam to the mass of the mixture, varies from near zero at the bottom of the generator to 17-33% in the riser just below the lower deck plate, depending on design and operating conditions. Such wet steam can not be send to the high pressure turbine. A special technology is required to remove the liquid from the steam as good as possible. Normally it happens in two stages: the first one removing the large size liquid and the second one removing the fine moisture – see Fig. 8.6. In Chap. 9 many details of separators design are given and methods haw to analyze their performance. Here only example is given on Figs. 8.2 and 8.5 where cylindrical primary separators are contained in a deck which seals the lower portion of the generator

containing the low quality steam from the upper portion containing the high quality steam.

The primary separators swirl the steam-water mixture so that the higher density water is thrown to the sides of the separator cylinder as a rising, rotating layer which is skimmed off. The mass carryover of water at the primary separator exit varies from 1 to 30%, again depending primarily on separator design. The water skimmed off flows from the deck into an annular down comer and is directed to the lower portion of the steam generator. There are several designs of cylindrical, centrifugal steam separators. Carson and Williams (1980) gives a compilation of various separator designs and their performance.

The secondary separators which are usually of a wire mesh or parallel vane design remove most of the remainder of the moisture from the steam. Gravity separation which may be relatively significant also occurs in the inter-space between the primary and secondary separators. The exit steam quality from present design steam generators is about 0.25%, while the design specifications for the recirculation ratio, and varies from 3 to 9 depending on steam separator and generator design. In such plants higher thermal efficiency is reached because the upper temperature is considerably higher. Besides the increase of the efficiency of the steam generators by using effective low pressure los high effective liquid separation technology the use of economizers is also important. Different type of economizers are in use: Economizers splitting the feed water flow with larger part send trough the cold part and smaller part trough the hot part. Other type of economizers called axial economizers sends the feed water trough the cold part only. Bussy et al. (1998) reported that sending the feed water trough the cold part only and redirecting 90% of the recirculation water to the hot part increases the steam pressure compared to steam generators of the design without these measures.

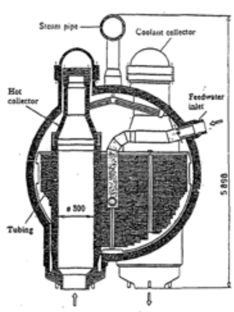

229.2 MWth, VVER-440

450 MWth, VVER-300/640 Ryjkov et al. (2009)

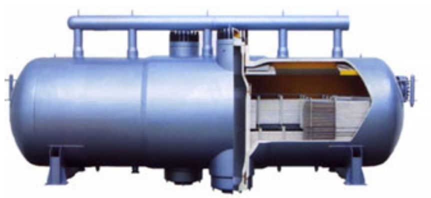

750 MWth, VVER-1000 SGSS (2009)

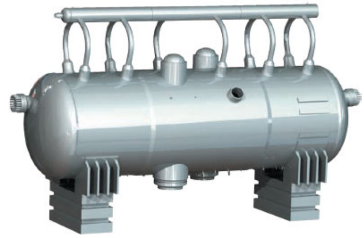

750-800 MWth, VVER-600/1000/1200 OKB (2008)

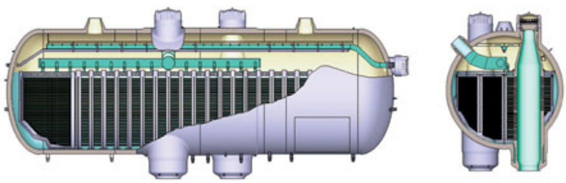

1062/1088 MWth VVER-1500/1600

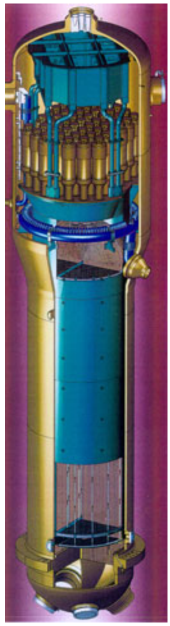

941 MWth, Konvoi

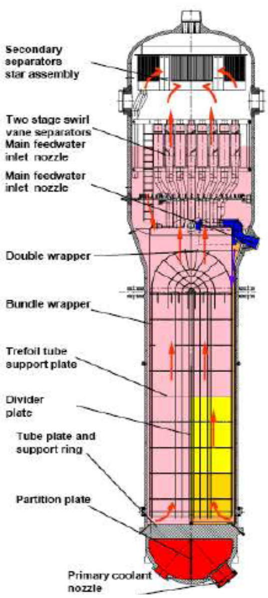

953-1100 MWth
ATMEA1 (2009)

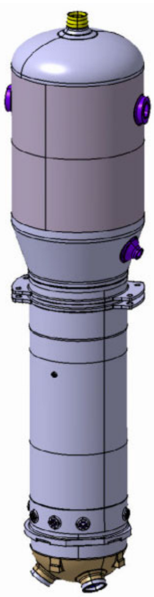

1131 MWth EPR
MNP (2009)

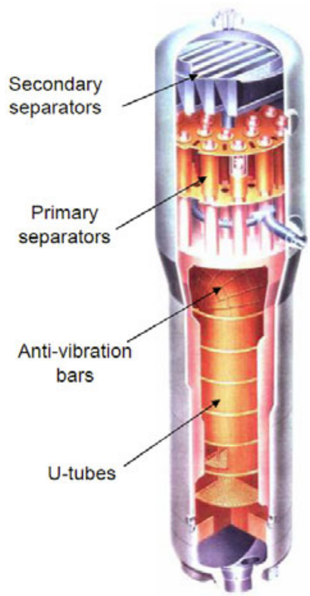

1113 MWth
US-APWR (2007d)

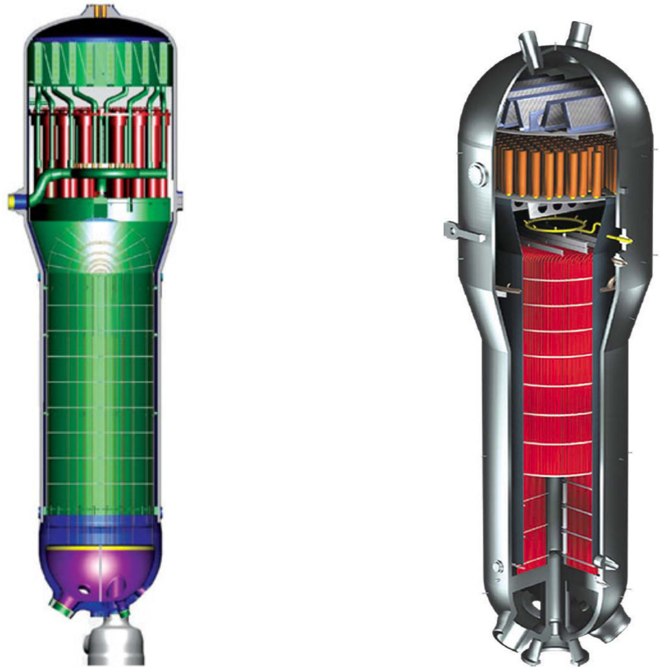

1707.5 MWth, AP1000 Cummins (2008) 2000 MWth, APR1400 (2009)

Fig. 8.7 The evolution of SG design

The evolution of the power per unit steam generator is demonstrated in Fig. 8.8 Starting with 229.2 MWth recently the order of 1700 - 2000 MWth is already achieved.

The Westinghouse, Combustion Engineering, Kraftwerk Union, Framatome and Mitsubishi designs have comparable operating parameters, while the Babcock & Wilcox/Atomic Energy of Canada Limited (B&W/AECL) design that will be discussed in the next section operates at lower temperatures and pressures.

8.2.2 Once through type

In the once trough steam generators (OTSG) from the type presented on Fig. 8.7 the heat transfer bundle is straight.

The primary fluid flows vertically downward trough straight vertical tubes, and the secondary fluid flows upwards outside the tubes. Feed water enters radially at the bottom and the superheated vapor with about 30K superheat exits radially near the top of the shell. This is the exciting feature of the OTSG – the possibility to superheat the steam. In the predominant part the use counter current flow principle provides good heat transfer efficiency. Some OTSG have either an economizer zone, other have some injection of steam in the secondary fluid about 1 to ½

of the height. This help to reach at lower elevation the saturation of the water and then to allow for superheating. These steam generators are simpler in design compared to the U-tube type. The secondary site heat transfer mechanism cross all regimes from the subcooled single phase convection to water to the single phase convection to steam. Especially endangered are the regions where the boiling crisis occurs because they naturally oscillate up and downwards around a given position causing thermal stresses. The film dry out leads to deposition of impurities at those places which change the heat transfer and accelerate corrosion.

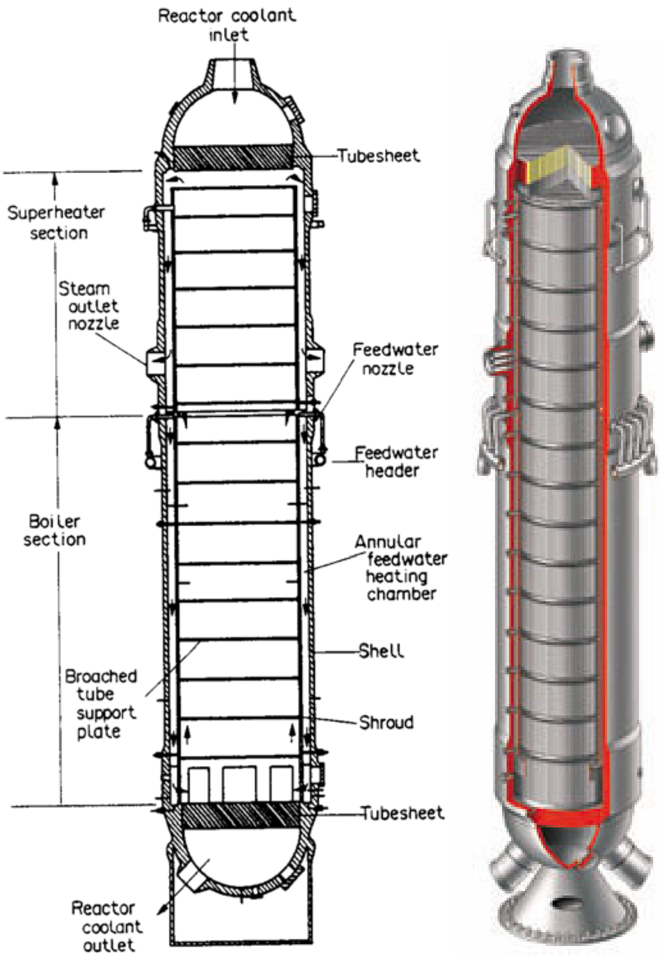

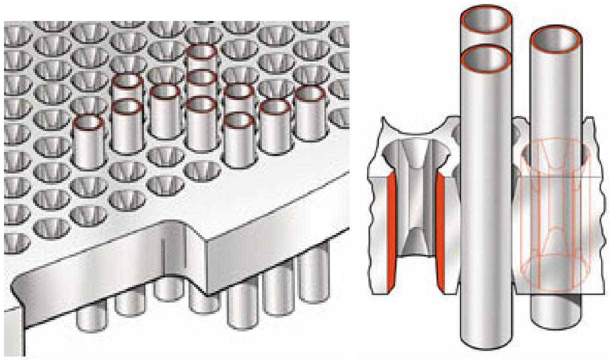

Fig. 8.8 Once through type steam generators for nuclear power plant: Babcoox and Wilcox design, Singhal and Srikantiah (1991), B&W (2009)

8.2.3 Other design types

Specific designs are known for nuclear power plants with different working principles then the pressurized water reactor. So for instance in pressurized heavy water reactors of the CANDU design the primary fluid is heavy water. Liquid metal cooled reactors such as the in Russian BN-600 reactor or the French Super Phoenix also use heat exchangers between primary very hot liquid metal coolant and at the secondary water coolant.

8.3 Frequent problems, sound design practices

If a tube bursts while a plant is operating contaminated steam could escape directly to the secondary cooling loop. Thus during scheduled maintenances, outages or shutdowns, some or all of the steam generator tubes are inspected by eddy-current testing or other means. If they are hermetic they are usually plugged, Keeton et al. (1986). An example is given in Fig. 8.9. After plugging more than a prescribed number of tubes the steam generator has to be replaced. This behavior is strongly influenced by the chemical water regime and the material selection.

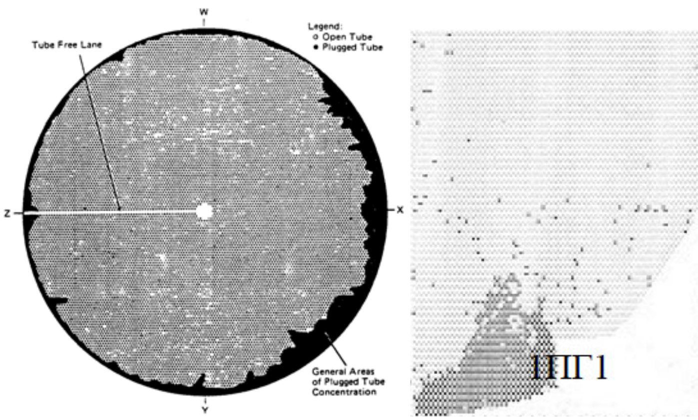

Fig. 8.9 Example of plugged tube concentration: a) vertical SG; b) horizontal SG

The usual problems with the steam generators leading to degradation are associated with vibration, fretting, fatigue, stress-corrosion, cracking, pitting, denting, deposition of corrosion products at the tube sheet etc., Green (1988), Solomon et al. (1985). So depending on the design, material selection and water chemistry the good steam generators already showed 30 years operation. Others loose their reliability after 15–20 years and are replaced. The deposition at the tube sheet reduces heat transfer surface and promote corrosion of the pipes. One should design such flow conditions that do not allow for intensive sedimentation of corrosion products on the tube sheet. High pressure water jets are usually used for cleaning this parts of the steam generator.

Bergunker VD (2006) reported that up to 2006 about 300 steam generators have been replaced. Each of the replacement costs between 30 and 100 millions, Wade (1995). In most of the cases thermal treated 690 Inconel alloy is used instead of 600MA Inconel alloy for the tubes, Trunov et al. (2008). In accordance with Trunov et al. (2008) up to 2008 there are 112 PGV-1000 and 162 PGV-440 horizontal steam generators in operation with 45 of PGV-1000 being replaced, Lukasevich et al. (2004) , Trunov et al. (2006).

Some sound design practices for vertical U-tube type steam generators are collected below:

1. Use 5 to 6 cylindrical forged elements and two heads: It reduces the weld length, reduces the ICI extend, reduces the radiation exposure of the personal by checking the welds.
2. Use integrally forged primary nozzles and man-ways to reduce required in-service inspissations.
3. Provide platforms around the SG for periodically checking the weldings.
4. Use of two level separation systems consisting of cyclones and dryers: It guarantees that the moisture is always less than the specified. The known components are tested by laboratory experiments and real operation.

5. Use of submerged in water feed water inlet and welded thermal sleeve: It protects against thermal stratification and thermal stress in the material.
6. Use of circumferential feed-water sparger in form of J-tubes with upper most openings. It prevents water hammer and dry out in case of low water level.
7. Use of corrosion resistant material for the pipes Incoloy 800: It prevents IGSCC and other material related corrosion. Select all other materials so as to minimize risk of primary water stress corrosion cracking, corrosion and erosion.
8. Use for the primary side 20 MnMoNi 5 5 and steal plated welding as the primary circuit;
9. Use for the tube support the Konvoi type egg-grid-type design: It minimizes the flow resistance, prevents deposits on the supports, there is no denting and no fretting. These egg-grids prove best behaviour in the practice compared to all other designs.
10. Use anti-vibration bar grids from Konvoi type;
11. Use a flow distribution baffle: It cause high velocity at the top of the tube sheet and therefore minimizes the deposits and reduces the risk of wastage and pitting.
12. Use for the tube to tube sheet connections welded into the primary side claddings and full depth of hydraulic expansion and two fold mechanical expansion. It prevents cruise corrosion;
13. Provide man hole in the primary and in the secondary side. Enhance access to internals of the secondary side for maintenance, tooling and foreign object search and retrieval coverage.
14. Provide an emergency discharge line from the steam space with upper most opening;
15. Provide high capacity emergency blow-down pipe from the bottom lane and a nozzle. It can be integrated with the tube sheet blow down line, which eliminates the need for separate internal blow down pipe;
16. Provide nozzles for chemical washing of the bottom secondary side.
17. Provide recirculation nozzles and associated piping and spargers for use during wet layup and cleaning.
18. Use integral channel head drains to drain primary fluid into reactor coolant system piping;
19. Use stand pipes and place the cyclones as high as technically possible. In this way the normal water level can be increased and therefore the power output. This increase the water amount in the secondary side and therefore the safety characteristics;
20. Use flexible support to allow normal operation considering thermal expansion and earthquake;
21. Design emergency feed water inlet;
22. The total SG height has to be between 20 and 24 m preferably 20 m;
23. Use forged tube sheet with integral cylindrical extension which provide better access underneath the peripheral tubes an and integrally forged primary nozzles and man ways to reduce the personal exposure by reducing the in-service inspection time;
24. Use electro polished surfaces for reduction of the personal exposure load;

25. Provide traps for loose-parts to avoid pipe damages;
26. Compare the sizes and the performance of the SG if based on 22 mm pipes with those based on 19 mm pipes (external diameter).
27. Introduce a peripheral channel in the low pressure side of the tube sheet in order to relax the thermal stresses and to facilitate easier slurry removal.
28. Use appropriate span of the narrow-range water-level taps to reduce the potential of reactor trips and provide increasing availability of viable water-level indication during and following upset conditions and certain accident scenarios;
29. Use loose-parts traps whenever possible and provide access to remove them.

Water level control: An important feature of the proper operation and protection of the plant is the water level control of the steam generator. The steam generator level control has to fulfill the following requirements:

1. To control the steam generator water level during start-up and shut-down, during full- and low- load operation with regard to load changes (step load changes, ramp load changes) including the associated transients;
2. To avoid any efficiency degradation of the moisture separators in case of rises in water level and to limit the associated increase in steam moisture content and therefore to protect the turbine;
3. To avoid an excessive steam generator feed after reactor trip;
4. To limit the rise of water level after restart of the reactor coolant pump;
5. To adjust the set point for the full-load and the low-load control downward in response to a steam generator tube leak for timely reduction of feed supply.

The parameters used as input variables for the design of the level control are; a) the measured changes in main steam flow rate; b) the measured changes in feed water supply; c) the changes in density following variation of measured pressures and temperatures.

The variation of the feed water flow is the action of the controller. Its can be organized with variable rotation speed of single pump or with combination of few pumps and changing the cross section of a valve after the pumps.

Wet steam moisture measurement:

Radioactive chemical tracers: EDF in cooperation with Stein-Industry uses the Dueymes (1989) method for moisture mass concentration measurements in nuclear power plants to control the efficiency of the separation devices. A water solution of lithium in hydroxide form (LiOH) and cesium in carbonate form (Cs_2CO_3) (radioactive tracer) is prepared in a vessel. Using a spectrophotometer, the mass concentration C_{inj} is measured. Then for a short period of time the tracer solution mass flow $\dot{m}_{inj}$ is injected into the wet steam line, preferably in a straight part where the disturbed turbulent velocity profile can recover after a 40-diameter travel path. At this position, samples are taken from the film part of the flow through a tapping hole. Then the concentration C_{film} is measured again using a

spectrophotometer. It is assumed that all the injected solution is homogeneously mixed in the flow due to the high level of turbulence so that the concentration in the flow $C_{flow} = C_{film}$ reaches much lower equilibrium values. Since the tracer mass remains constant,

$$\dot{m}_{inj} C_{inj} = \left(\dot{m}_{liquid} + \dot{m}_{inj} \right) C_{film} , \tag{8.1}$$

the liquid mass is easily computed to be

$$\dot{m}_{liquid} = \dot{m}_{inj} \left(C_{inj} / C_{film} - 1 \right) , \tag{8.2}$$

and therefore the mass concentration of steam in the steam–liquid mixture is given by

$$X_1 = \dot{m}_{steam} / \left(\dot{m}_{liquid} + \dot{m}_{steam} \right) . \tag{8.3}$$

Of course, knowledge of the steam mass flow $\dot{m}_{steam}$ is needed to use the method.

Using the above method, nuclear steam supply facilities are sometimes tested by injecting radioactive tracers into the feed water *before* the steam generator. It is assumed that the tracers are carried over only in the water droplets, so the percentage residual radioactivity is assumed to be equal to the percent moisture in the steam supply out of the steam generator. A large bureaucratic effort is needed to receive permission for such a test. In nuclear plants, this measurement is done once or twice in their lifetime. That is why methods are developed that use nonradioactive chemical tracers.

Nonradioactive chemical tracers: Sodium sulfate at 5 ppb or less is usually used. In general the safety requirements dictate that if the concentration exceeds 50 ppb the plant power has to be reduced and the source of the contaminant has to be identified. An example is given below for a two-loop PWR for the estimation of the moisture concentration for steam generators without economizers.

Task: We know the recirculation ratio r of both steam generators (SG1, SG2) and their feed water mass flows, $\dot{m}_{feed\_water,SG1}$, $\dot{m}_{feed\_water,SG2}$, which can be assumed equal to the steam–water mixture mass flow produced by SG1 and SG2, $\dot{m}_{steam\_water\_mixture,SG1}$, $\dot{m}_{steam\_water\_mixture,SG2}$, respectively. We have measured the ratios of the concentrations of the feed water $C_{feed\_water,i}$ and of the blow down pipe $C_{blow\_down,i}$, $C_{feed\_water,i} / C_{blow\_down,i}$, and the ratios of the steam–water mass concentration of SG2 $C_{steam\_water\_mixture,SG2}$ and SG1 $C_{steam\_water\_mixture,SG1}$, $C_{steam\_water\_mixture,SG2} / C_{steam\_water\_mixture,SG1}$, respectively. Note that not absolute values but ratios of concentrations are required, which are accurately measurable. Estimate the moisture mass concentration in the exit mixture of SG1, $X_{2,steam\_water\_mixture,SG1}$.

Solution: This is proposed by Fournier et al. (2009). The liquid mass concentration in the water–steam mixture at the exit of the *i*th steam generator is defined as follows:

$$X_{2,steam\_water\_mixture,SGi} = \frac{C_{steam\_water\_mixture,SGi}}{C_{riser\_mixture,SGi}} . \tag{8.4}$$

Consequently for two steam generators we have

$$\frac{X_{2,steam\_water\_mixture,SG2}}{X_{2,steam\_water\_mixture,SG1}} = \frac{C_{riser\_mixture,SG1} C_{steam\_water\_mixture,SG2}}{C_{riser\_mixture,SG2} C_{steam\_water\_mixture,SG1}} . \tag{8.5}$$

The tracer mass conservation equation for both steam generators is

$$\dot{m}_{steam\_water\_mixture,SG1} C_{steam\_water\_mixture,SG1} + \dot{m}_{steam\_waer\_mixture,SG2} C_{steam\_waer\_mixture,SG2}$$

$$= \left(\dot{m}_{feed\_water,SG1} + \dot{m}_{feed\_water,SG2} \right) C_{feed\_water} . \tag{8.6}$$

Placing Eq. (8.4) into Eq. (8.6) results in

$$\dot{m}_{steam\_water\_mixture,SG1} X_{2,steam\_water\_mixture,SG1} C_{riser\_mixture,SG1}$$

$$+ \dot{m}_{steam\_waer\_mixture,SG2} X_{2,steam\_water\_mixture,SG2} C_{riser\_mixture,SG2}$$

$$= \left(\dot{m}_{feed\_water,SG1} + \dot{m}_{feed\_water,SG2} \right) C_{feed\_water} . \tag{8.7}$$

Using Eq. (8.5) the above equation transforms into

$$\boxed{X_{2,steam\_water\_mixture,SG1} = \frac{\left(\dot{m}_{feed\_water,SG1} + \dot{m}_{feed\_water,SG2} \right) C_{feed\_water}}{\left(\dot{m}_{steam\_water\_mixture,SG1} + \dot{m}_{steam\_water\_mixture,SG2} \dfrac{C_{steam\_water\_mixture,SG2}}{C_{steam\_water\_mixture,SG1}} \right) C_{riser\_mixture,SG1}} .} \tag{8.8}$$

The riser tracer concentration is difficult to measure. It is easier to measure the blow down concentration. From the tracer mass conservation before and after the mixing,

$$\dot{m}_{riser,SGi} C_{riser\_mixture,SGi} = \left(\dot{m}_{riser,SGi} + \dot{m}_{feed\_water,SGi} \right) C_{blow\_down,i} , \tag{8.9}$$

the riser mass concentration can be expressed as a function of the blow down concentration

$$C_{riser\_mixture,SGi} = \frac{\dot{m}_{riser,SGi} + \dot{m}_{feed\_water,SGi}}{\dot{m}_{riser,SGi}} C_{blow\_down,i}, \tag{8.10}$$

assuming that the recirculation ratio

$$r = \frac{\dot{m}_{riser,SGi} + \dot{m}_{steam\_water\_mixture,SGi}}{\dot{m}_{steam\_water\_mixture,SGi}} = 1 + \frac{\dot{m}_{riser,SGi}}{\dot{m}_{steam\_water\_mixture,SGi}} \tag{8.11}$$

is known. From this definition of the recirculation ratio we compute the riser mass flow:

$$\dot{m}_{riser,SGi} = (r-1)\dot{m}_{steam\_water\_mixture,SGi}. \tag{8.12}$$

With this and assuming that at steady state the feed-water mass flow is equal to the steam mixture flow leaving the steam generator,

$$\dot{m}_{steam\_water\_mixture,SGi} = \dot{m}_{feed\_water,SGi}, \tag{8.13}$$

Eq. (8.10) can be rewritten as

$$C_{riser\_mixture,SGi} = \frac{1}{r-1} \frac{\dot{m}_{riser,SGi} + \dot{m}_{feed\_water,SGi}}{\dot{m}_{steam\_water\_mixture,SGi}} C_{blow\_down,i} = \frac{r}{r-1} C_{blow\_down,i}. \tag{8.14}$$

With this, Eq. (8.8) receives finally the form

$$\boxed{X_{2,steam\_water\_mixture,SG1} = \frac{r-1}{r} \frac{C_{feed\_water}}{C_{blow\_down,i}} \frac{\dot{m}_{feed\_water,SG1} + \dot{m}_{feed\_water,SG2}}{\dot{m}_{steam\_water\_mixture,SG1} + \dot{m}_{steam\_water\_mixture,SG2} \dfrac{C_{steam\_water\_mixture,SG2}}{C_{steam\_water\_mixture,SG1}}}.} \tag{8.15}$$

This is the final expression, Eq. (8.10) by Fournier et al. (2009), used for estimation of the moisture mass concentration at the exit of SG1. Note that the blow down mass flow must be low enough (< 5000–10 000 pound mass per hour) not to change the concentrations in the steam generator.

Calorimetric method: Another method for measuring the steam quality is the calorimetric method based on isokinetic removal of steam–water mixture from a given position of the pipe cross-section. After the reducing the pressure in a

perfectly thermally isolated device and measuring the temperature and pressure before and after the discharge, the equality of the enthalpies,

$$X_1 h''(p) + (1 - X_1) h'(p) = h(T_{reduces}, p_{reduced}), \tag{8.16}$$

gives the moisture mass concentration

$$1 - X_1 = 1 - \left[h(T_{reduces}, p_{reduced}) - h'(p) \right] / \left[h''(p) - h'(p) \right]. \tag{8.17}$$

This is an extremely sensitive method and requires careful device design. Several conditions have to be fulfilled to obtain appropriate local moisture measurement: (a) the removed mass flow has to be taken at zero pressure difference along the removal line (isokinetic removal) – this has to be adjusted during the removal by adjusting the hydraulic resistance of the removal channel; (b) the film flow has to be negligible; (c) the device has to offer the possibility to trace the pipe cross-section in order to measure the moisture contentment over the cross-section. Integration is then possible if the local velocity is also simultaneously measured. A successful device based on this principle was developed, applied, and reported by Rütz (1973).

8.4 Analytical tools

8.4.1 Some preliminary remarks on the physical problem to be solved

In designing modern steam generators the following thermal-hydraulic task has to be solved.

Given are:

(a) the prescribed geometry, e.g., number of heat-exchanging pipes n_p, heat transfer surface from the secondary side $F_{ht,II}$, internal diameter $D_{p,in}$ and wall thickness δ_p of the pipes corresponding to average pipe length $L_{p,av}$;

(b) their geometrical arrangement in a vessel, size and geometry of the vessel, design characteristics of separation devices like cyclones and dryers, etc.;

(c) the mass flow of the primary circuit $\dot{m}_{I,in}$ with its corresponding inlet temperature $T_{2,I,in}$ and pressures $p_{I,in}$, and eventually vapor mass flow ratio $X_{1,I,in}$, which corresponds to the void fraction $\alpha_{1,I,in}$;

(d) the allowable exit coolant temperature $T_{2,I,out}$,

(e) the inlet temperature of the feed water $T_{2,II,in}$.

Compute:

(a) the thermal power $\dot{Q}$ that can be removed from the primary circuit for a given controlled water level $L_{II,opt}$;
(b) the inlet feed-water mass flow, $\dot{m}_{II,in}$;
(c) the produced steam mass flow $\dot{m}_{II,out}$;
(d) the pressure in the dome for a prescribed exit pressure after the steam nozzle p_{II} ;
(e) the recirculation ratio r_{II} .

Note that the so-called recirculation ratio r_{II} is then the mass flow entering the bundle $\dot{m}_{II,in} + \dot{m}_r$, divided by the produced steam mass flow $\dot{m}_{II,out}$,

$$r_{II} = \frac{\dot{m}_{II,in} + \dot{m}_r}{\dot{m}_{II,out}} .$$

Here $\dot{m}_{II,in}$ is the feed-water mass flow and $\dot{m}_r$ is the mass flow returned by the cyclones and dryers and mixed with the feed-water flow. In the following a lumped-parameter order-of-magnitude estimate is given.

8.4.2 Some simple conservation principles

The steady-state mass conservation of the secondary side of the SG says that the feed-water mass flow is equal to the produced steam mass flow.

$$\dot{m}_{II,in} = \dot{m}_{II,out} .$$

The total energy conservation of the SG says that the inlet energy plus the thermal input is equal to the energy leaving the system:

$$\dot{m}_{II,in} h_{II,in} + \dot{Q} = \dot{m}_{II,out} h_{II,out} \text{ or } \dot{Q} = \dot{m}_{II,in} \left(h_{II,out} - h_{II,in} \right) .$$

Here the feed-water mass flow in kg/s is $\dot{m}_{II,in}$, the corresponding specific enthalpy in J/kg is $h_{II,in} = h\left(p_{II}, T_{II,in} \right)$, the thermal power transmitted from the primary to the secondary fluid in W is $\dot{Q}$, the steam mass flow in kg/s is $\dot{m}_{II,out}$, and finally the specific enthalpy of the steam in J/kg is $h_{II,out} = h''\left(p_{II} \right)$, which is

usually set to the saturation enthalpy at the system pressure. Solving with respect to the feed-water mass flow results in

$$\boxed{\dot{m}_{II,in} = \frac{\dot{Q}}{h_{II,out} - h_{II,in}} = \frac{\dot{Q}}{h''(p_{II}) - h\left(p_{II}, T_{II,in}\right)}.}$$

The recirculation mass flow in kg/s is designated $\dot{m}_r$. As already mentioned, the so-called recirculation ratio r_{II} is then the mass flow entering the bundle divided by the produced steam mass flow. Therefore the recirculation mass flow is

$$\dot{m}_r = r_{II}\dot{m}_{II,out} - \dot{m}_{II,in} = \left(r_{II} - 1\right)\dot{m}_{II,in}.$$

The mass flow trough the bundle is therefore

$$\boxed{\dot{m}_r + \dot{m}_{II,in} = r_{II}\dot{m}_{II,in}.}$$

The steam quality at the exit of the bundle is computed from the energy balance of the riser (bundle region) only

$$\left(\dot{m}_r + \dot{m}_{II,in}\right)\left[X_{II,1}h''(p_{II}) + \left(1 - X_{II,1}\right)h'(p_{II})\right] = \dot{m}_r h'(p_{II}) + \dot{m}_{II,in}h_{II,in} + \dot{Q},$$

resulting in

$$\boxed{X_{II,1} = \frac{\dot{Q}/\dot{m}_{II,in} + h_{II,in} - h'(p_{II})}{r_{II}\left[h''(p_{II}) - h'(p_{II})\right]} = \frac{h_{II,out} - h'(p_{II})}{r_{II}\left[h''(p_{II}) - h'(p_{II})\right]} = \frac{1}{r_{II}}.}$$

Obviously increasing the recirculation ratio decreases the steam quality at the exit, which is important information for designing the water separation devices.

Having these relations the mixing enthalpy at the entrance of the bundle is easily computed:

$$h_{mix} = \frac{\dot{m}_r h_r + \dot{m}_{II,in}h_{II,in}}{\dot{m}_r + \dot{m}_{II,in}} = h_r - \left(h_r - h_{II,in}\right)\frac{\dot{m}_{II,in}}{r_{II}\dot{m}_{II,out}}$$

$$= h_r + \left(\frac{h_r}{h_{II,in}} - 1\right)\left(\frac{\dot{Q}}{r_{II}\dot{m}_{II,out}} - \frac{h_{II,out}}{r_{II}}\right)$$

$$= h'(p_{II}) + \frac{1}{r_{II}}\left(\frac{h'(p_{II})}{h\left(p_{II}, T_{II,in}\right)} - 1\right)\left(\frac{\dot{Q}}{\dot{m}_{II,out}} - h''(p)\right).$$

Here the specific enthalpy belonging to the recirculation mass flow in J/kg is $h_r = h'\left(p_{II}\right)$. Therefore the mixing enthalpy is a function of five parameters:

$$h_{mix} = h_{mix}\left(p_{II}, \dot{Q}, \dot{m}_{II,out}, T_{2,II,in}, r_{II}\right).$$

In reality it is a complicated function of the space also because of the type of feed-water introduction and the separated moisture deposition in the down-comer.

While the assumption of thermodynamic equilibrium is an acceptable simplification for microscopic balances, the assumption of homogeneous intermixing is a rough approximation. In fact for large steam generators, there are heterogeneities in the supply of separated water and of the feed water, and very strong heterogeneities in the generating the steam along and across the riser. Therefore 3D analysis is necessary. Furthermore, the mass flow trough the riser is a function of the adjustment of the mechanical equilibrium: driving forces equal to the resistance forces. In addition the water level is controlled at a specified level which imposes the component of the driving forces in the down-comer. The resisting forces then turn control the riser mass flow itself:

$$\dot{m}_{II,bundle} = f\left[\Delta p_{beouancy}\left(\dot{m}_{II,bundle},...\right), \Delta p_{friction}\left(\dot{m}_{II,bundle},...\right), Water\ level\right].$$

8.4.3 Three-dimensional analysis

Actually the method of the multiphase flow analysis as described in this monograph is what is needed to analyze the processes inside the steam generators. Usually the porous body concept is used in which with surface permeabilities and porosities describe the secondary control volume reduction due to tubes and flow obstacles, see Appendix 1. An example is given in Fig. 8.10(a). The primary side is described as a multiple of a representative pipe starting from the inlet plenum and ending at the outlet plenum. The thermal coupling is then arranged between corresponding primary and secondary control volumes through transient heat conduction. It is important to have models for boiling including the boiling creases with the logic of adjustable heat fluxes at both sides. After reaching the critical heat flux the transition boiling is entered, up to the minimum film boiling temperature. Then by further increasing the power, transition to film boiling is in place. There is no hysteresis in the boiling curve. Note the difference to nuclear heating. The modeling of the separators can happen at different levels of complexity: use of experimental characteristics inside the control volumes and transmitting of the separated liquid and gas in other volumes; use in the same way of analytically derived characteristics as described in Chap. 9; use of fine resolution with boundary fitted coordinates for the separators and therefore natural modeling of the entrained liquid and gas. The last method is the most expensive and still not in use. Note that the integral characteristics of the final steam are of interest. Recirculation ratio, temperature and void distribution, pressure level at

given steam mass flow, etc. are usually requested as output of thermohydraulic analysis. Figure 8.10(b) gives an illustration of a numerically obtained solution for the steam generator with geometry presented in Fig. 8.2. The fascinating feature of the multifluid computational analysis is that it provides the local void distribution, the velocity fields, the vibration characteristics, etc.

General verification of multiphase models is usually combined with prediction using a limited number of heat exchanger and model steam generator experiments, Fortino et al. (1980), Singhal et al. (1984), Wang and Srikantiah (1985), Lee and No (1986), Aubry et al. (1989), Keeton et al. (1990), Singhal and Srikantiah (1991), John et al. (2005). Data are reported by Gautier and Boissier (1971), Riboud and Brugeille (1987), Gouirand (1989, 1991) for heat exchangers. A numerical example given by Patankar and Spalding (1976) can be used as a benchmark for single-phase flow. Tests for model steam generators are discussed by Singhal et al. (1983). Hassan and Morgan (1980) compared their analysis with a well-documented simple boiler experiment. Finally, the best way of confirming the design is to equip a real steam generator with measurements and to take its relevant characteristics during the operation in a real plant: Procaccia et al. (1982), Carlucci et al. (1982) compared their analysis with data collected on a real industrial steam generator of a US nuclear power plant. Schwarz and Bouecke (1985) compared their analysis with data collected on a real industrial steam generator of a German nuclear power plant. Bussy et al. (1998) compared their analysis with data collected on a real industrial steam generator (N4) of French nuclear power plants.

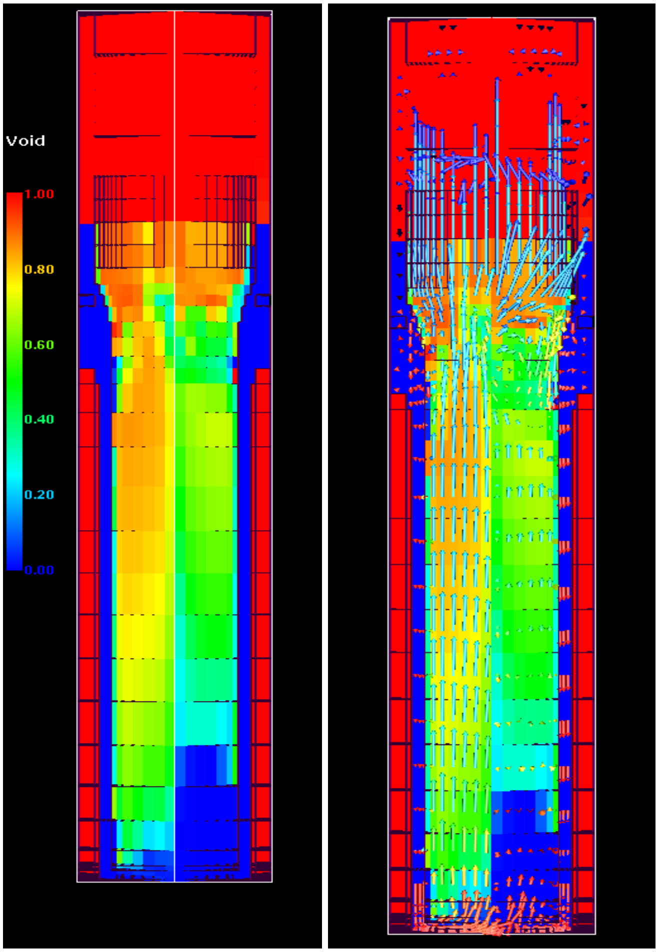

(a) (b)

Fig. 8.10 Computational model of the secondary side of a steam generator using the IVA porous body concept: (**a**) void fraction at steady state as a function of space: *right* – cold side, *left* – hot side, *blue* – pure water, *red* – pure steam; (**b**) velocity of liquid as a function of space

8.5 Validation examples

8.5.1 Benchmark for heat exchanger design with complex computer codes

The subject of this section is to define examples of heat exchangers that can be easily solved. The solution obtained can then be used for check the performance of complex models in computer codes.

Problem 1: A heat exchanger consists of a bundle of n_{pipes} pipes placed in a large-diameter pipe. The internal diameter of the heat transfer pipes is $2R_1$, the external $2R_2$. The heated diameter of the primary side is therefore $D_{heat,1} = 2R_1$. The wand thickness is δ_w. The length of the pipes is $L_{pipes} = 6.38$ m. The diameter of the secondary side pipe is D_{vessel}. The flow cross-section of the secondary side is equal to $\frac{\pi}{4}D_{vessel}^2 - n_{pipes}\pi R_2^2$. Usually the high-pressure medium is flowing through the small-diameter pipes for economic reasons. The pressure at the inlet is equal to 150 bar and the temperature 90°C. The pressure at the inlet in the secondary side is 7 bar and the temperature 38°C. Some thermodynamic properties at these conditions are: High pressure inlet: ρ_1 = 972.99 kg/m³, c_{p1} = 4173 J/(kg K), η_1 = 318.4E-6 kg/(m s), λ_1 = 0.683 W/(m K); Low pressure: ρ_2 = 993.23 kg/m³, c_{p2} = 4177 J/(kg K), η_2 = 678.3E-6 kg/(m s), λ_2 = 0.628 W/(m K). For the geometry summarized below, compute the parameter distribution along the flow and the power of the heat exchanger for parallel flow.

Summary of the geometrical data and initial conditions:

L_{pipes} = 6.38 m, Δz = 0.0638 m, δ_w = 0.0024 m, R_1 = 0.005 m, $R_2 = R_1 + \delta_w$, n_{pipes} = 259, R_{vessel} = 0.155 m, $D_{heat,1}$ = 0.01 m, $D_{heat,2} = 4\left(R_{vessel}^2 - n_{pipes}R_2^2\right)/\left(n_{pipes}2R_2\right)$,
$D_{hyd,1}$ = 0.01 m, $D_{hyd,2} = 4\left(R_{vessel}^2 - n_{pipes}R_2^2\right)/\left(n_{pipes}2R_2 + 2R_2\right)$, w_1 = 0.9 m/s, w_2 = 0.706 m/s, $T_{1,in}$ = 363.15 K, $T_{2,in}$ = 311.15 K, λ_w = 44.713 W/(m K).

Note that the vessel size has to be selected such that the flow cross-section is a positive number, $F_2 = \pi\left(R_{vessel}^2 - n_{pipes}R_2^2\right) > 0$.

Solution: The steady-state energy conservation equations for the primary and secondary fluids are

$$\rho_1 w_1 c_{p1} \frac{dT_1}{dz} = -\frac{4}{D_{heat,1}} h_{1w} \left(T_1 - T_{1w} \right),$$

$$\rho_2 w_2 c_{p2} \frac{dT_2}{dz} = \frac{4}{D_{heat,2}} h_{2w} \left(T_{2w} - T_2 \right).$$

The heat fluxes at the primary and secondary sides satisfy the Fourier equation

$$\dot{q}''_{1w} = h_{1w} \left(T_1 - T_{1w} \right) = \frac{1}{R_1} \frac{T_{1w} - T_{2w}}{R_w},$$

$$\dot{q}''_{w2} = h_{2w} \left(T_{2w} - T_2 \right) = \frac{1}{R_2} \frac{T_{1w} - T_{2w}}{R_w},$$

where

$$R_w = \frac{1}{\lambda_w} \ln \frac{R_2}{R_1}.$$

The wall temperatures can be excluded from the following equation system:

$$\begin{pmatrix} 1 + R_1 R_w h_{1w} & -1 \\ 1 & -\left(1 + R_2 R_w h_{2w}\right) \end{pmatrix} \begin{pmatrix} T_{1w} \\ T_{2w} \end{pmatrix} = \begin{pmatrix} R_1 R_w h_{1w} T_1 \\ -R_2 R_w h_{2w} T_2 \end{pmatrix},$$

resulting in

$$T_{1w} = \left[-R_1 R_w h_{1w} T_1 \left(1 + R_2 R_w h_{2w}\right) - R_2 R_w h_{2w} T_2 \right] / D,$$

$$T_{2w} = \left[-\left(1 + R_1 R_w h_{1w}\right) R_2 R_w h_{2w} T_2 - R_1 R_w h_{1w} T_1 \right] / D,$$

where

$$D = 1 - \left(1 + R_1 R_w h_{1w}\right)\left(1 + R_2 R_w h_{2w}\right).$$

Therefore the difference of the temperature at both sides is

$$T_{1w} - T_{2w} = R_w k \left(T_1 - T_2 \right),$$

where

$$k = \frac{1}{R_w + \dfrac{1}{R_1 h_{1w}} + \dfrac{1}{R_2 h_{2w}}} .$$

Therefore the heat fluxes can be expressed as a function of the fluid temperature difference:

$$\dot{q}''_{1w} = \frac{k}{R_1}\left(T_1 - T_2\right) ,$$

$$\dot{q}''_{w2} = \frac{k}{R_2}\left(T_1 - T_2\right) .$$

With this the energy conservation equations simplify to

$$\frac{dT_1}{dz} = -a\left(T_1 - T_2\right) ,$$

$$\frac{dT_2}{dz} = b\left(T_1 - T_2\right) ,$$

where $a = 4k\big/\left(D_{heat,1} R_1 \rho_1 w_1 c_{p1}\right)$ and $b = 4k\big/\left(D_{heat,2} R_2 \rho_2 w_2 c_{p2}\right)$. Writing in finite difference form for co-current flows,

$$T_{1,i} - T_{1,i-1} = -\frac{1}{2} a \Delta z \left(T_{1,i-1} + T_{1,i} - T_{2,i-1} - T_{2,i}\right) ,$$

$$T_{2,i} - T_{2,i-1} = \frac{1}{2} b \Delta z \left(T_{1,i-1} + T_{1,i} - T_{2,i-1} - T_{2,i}\right) ,$$

for each particular point we obtain the system of algebraic equations

$$\begin{pmatrix} 1 + \frac{1}{2} a \Delta z & -\frac{1}{2} a \Delta z \\ -\frac{1}{2} b \Delta z & 1 + \frac{1}{2} b \Delta z \end{pmatrix} \begin{pmatrix} T_{1,i} \\ T_{2,i} \end{pmatrix} = \begin{pmatrix} \left(1 - \frac{1}{2} a \Delta z\right) T_{1,i-1} + \frac{1}{2} a \Delta z T_{2,i-1} \\ \frac{1}{2} b \Delta z T_{1,i-1} + \left(1 - \frac{1}{2} b \Delta z\right) T_{2,i-1} \end{pmatrix} ,$$

which is then solved with respect to the unknown point temperature moving from the inlet to the outlet. To compute the heat transfer coefficients we need the *Reynolds* and the *Prandtl* numbers for both flows. Assuming constant properties equal at those at the entrance we have $\mathrm{Re}_1 = \rho_1 w_1 D_{1,hyd} / \eta_1$, $\mathrm{Re}_2 = \rho_2 w_2 D_{2,hyd} / \eta_2$, $\mathrm{Pr}_1 = \eta_1 c_{p1} / \lambda_1$, $\mathrm{Pr}_2 = \eta_2 c_{p2} / \lambda_2$. With this the *Nusselt* numbers are

$Nu_1 = 0.023\mathrm{Re}_1^{0.8}\mathrm{Pr}_1^{1/3}$ and $Nu_2 = 0.023\mathrm{Re}_2^{0.8}\mathrm{Pr}_2^{1/3}$, and the corresponding heat transfer coefficients $h_{1w} = Nu_1\lambda_1/D_{1,hyd}$ and $h_{2w} = Nu_2\lambda_2/D_{2,hyd}$, respectively. The result for our particular case is Re_1 = 27474, Re_2 = 9823, Pr_1 = 1.94, Pr_2 = 4.51, Nu_1 = 102, Nu_2 = 59, h_{1w} = 6977, h_{2w} = 3925, k = 13.9, a = 1.945E-02, and b = 1.595E-02.

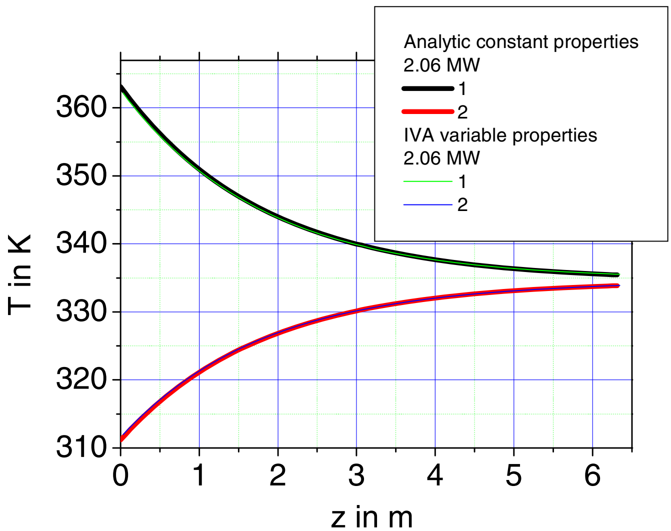

Fig. 8.11 Temperatures along the pipes for both sides of co-current heat exchangers

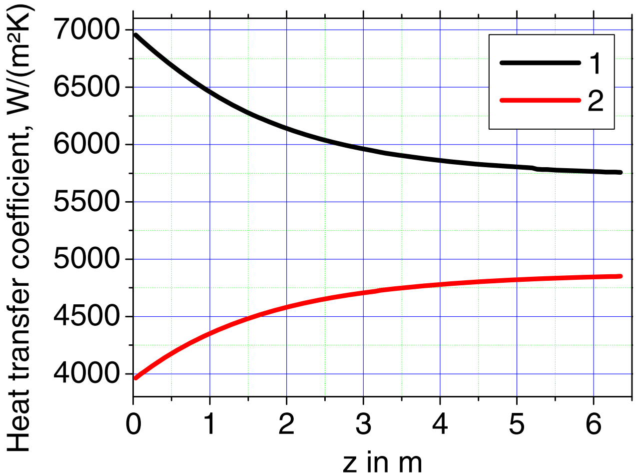

Fig. 8.12 Heat transfer coefficients at both sides as functions of the spatial coordinate

Figure 8.11 gives the temperatures of the fluid at both sides for co-current flow heat exchanger. In the same figure are given the predictions of the IVA computer code. We see excellent agreement. The computed power for the analytical benchmark is

$$\dot{Q}_{1w} = n_{pipes}\pi 2R_1\Delta z\sum \dot{q}''_{1w} = n_{pipes}\pi 2R_1\Delta z\frac{k}{R_1}\sum\left(T_1 - T_2\right) = n_{pipes}\pi 2\Delta z k\sum\left(T_1 - T_2\right),$$

$$\dot{Q}_{2w} = n_{pipes}\pi 2R_2\Delta z\sum \dot{q}''_{2w} = n_{pipes}\pi 2R_2\Delta z\frac{k}{R_2}\sum\left(T_1 - T_2\right) = n_{pipes}\pi 2\Delta z k\sum\left(T_1 - T_2\right).$$

and in this particular case 2.060291 MW. The computed power using the computer code is then 2.06107 MW. Note that in reality the heat transfer coefficients are not constant, as demonstrated in Fig. 8.12 by the IVA code predictions. This explains the slight difference in the computed powers.

Of course the well-known analytical solution of this problem reported by Miheev and Miheeva (1973) p. 238 can also be used, applying it for each spatial interval: Subtracting both energy conservation equations results in a single ordinary differential equation with respect to the driving temperature difference:

$$d\ln\left(T_1 - T_2\right) = -\left(a + b\right)dz,$$

having the solution $\ln \frac{T_{1,i} - T_{2,i}}{T_{1,i-1} - T_{2,i-1}} = -(a+b)\Delta z$ or

$$\frac{T_{1,i} - T_{2,i}}{T_{1,i-1} - T_{2,i-1}} = \exp\left[-(a+b)\Delta z\right].$$

Subtracting from unity both sides of the above equation results in the equality

$$1 - \frac{T_{1,i} - T_{2,i}}{T_{1,i-1} - T_{2,i-1}} = 1 - \exp\left[-(a+b)\Delta z\right],$$

or

$$T_{1,i-1} - T_{1,i} + T_{2,i} - T_{2,i-1} = \left(T_{1,i-1} - T_{2,i-1}\right)\left\{1 - \exp\left[-(a+b)\Delta z\right]\right\}.$$

Considering that the thermal energy removed from the primary side $\rho_1 w_1 F_1 c_{p1} dT_1 = -\dot{Q}_{12}$ is inserted into the secondary side $\rho_2 w_2 F_2 c_{p2} dT_2 = \dot{Q}_{12}$, resulting in

$$T_{2,i} - T_{2,i-1} = \frac{\rho_1 w_1 F_1 c_{p1}}{\rho_2 w_2 F_2 c_{p2}}\left(T_{1,i-1} - T_{1,i}\right),$$

which combined with the above equation gives the temperature change in the primary side,

$$\boxed{T_{1,i-1} - T_{1,i} = \left(T_{1,i-1} - T_{2,i-1}\right)\frac{\left\{1 - \exp\left[-(a+b)\Delta z\right]\right\}}{1 + \dfrac{\rho_1 w_1 F_1 c_{p1}}{\rho_2 w_2 F_2 c_{p2}}},}$$

the temperature change of the secondary-side fluid is then

$$\boxed{T_{2,i} - T_{2,i-1} = \left(T_{1,i-1} - T_{2,i-1}\right)\frac{\left\{1 - \exp\left[-(a+b)\Delta z\right]\right\}}{1 + \dfrac{\rho_1 w_1 F_1 c_{p1}}{\rho_2 w_2 F_2 c_{p2}}}\frac{\rho_1 w_1 F_1 c_{p1}}{\rho_2 w_2 F_2 c_{p2}}.}$$

Problem 2: Given the problem described above, develop a simple model for transient heat transfer across the heat-conducting pipe by taking into account its thermal inertia.

Solution: We first define a temperature T_w^* at the middle of the pipe at $R^* = R_1 + \delta_w/2$. The steady-state heat flux from medium 1 to the middle of the pipe and from the middle of the pipe to medium 2 is

$$\dot{q}''_{1w} = h_{1w}\left(T_1 - T_{1w}\right) = \frac{1}{R_1}\frac{T_{1w} - T_w^*}{R_{w1}^*} = \frac{h_{1w}}{k_1^*}\left(T_1 - T_w^*\right),$$

$$\dot{q}''_{w2} = h_{2w}\left(T_{2w} - T_2\right) = \frac{1}{R_2}\frac{T_w^* - T_{2w}}{R_{w2}} = \frac{h_{2w}}{k_2^*}\left(T_w^* - T_2\right),$$

respectively, where

$$R_{w1}^* = \frac{1}{\lambda_w}\ln\frac{R^*}{R_1},\ k_1^* = h_{1w}R_1R_{w1}^* + 1,$$

$$R_{w2}^* = \frac{1}{\lambda_w}\ln\frac{R_2}{R^*},\ k_2^* = h_{2w}R_2R_{w2}^* + 1.$$

The energy conservation equation for the pipe segment with length 1 m is

$$\frac{1}{2}\rho_w c_{pw}\left(R_2^2 - R_1^2\right)\frac{dT_w^*}{d\tau} = \frac{R_1h_{1w}}{k_1^*}\left(T_1 - T_w^*\right) - \frac{R_2h_{2w}}{k_2^*}\left(T_w^* - T_2\right).$$

The steady-state structure temperature is

$$T_{w\infty}^* = \left(h_{1w}R_1T_1/k_1^* + h_{2w}R_2T_2/k_2^*\right)\Big/\left(h_{1w}R_1/k_1^* + h_{2w}R_2/k_2^*\right).$$

The time constant of the process is

$$\Delta\tau_w^* = \frac{1}{2}\rho_w c_{pw}\left(R_2^2 - R_1^2\right)\Big/\left(h_{1w}R_1/k_1^* + h_{2w}R_2/k_2^*\right).$$

With this the energy conservation for a pipe section can then be written in simple form,

$$\Delta\tau_w^*\frac{dT_w^*}{d\tau} = \left(T_{w\infty}^* - T_w^*\right),$$

with the solution for the time interval $\Delta\tau$

$$T_w^* = T_{w\infty}^* + \left(T_{w,old}^* - T_{w\infty}^*\right)\Big/\exp\left(\Delta\tau/\Delta\tau_w^*\right).$$

Having the new temperature at the middle of the wall the heat fluxes are $\dot{q}''_{1w} = h_{1w}\left(T_1 - T_w^*\right)/k_1^*$ and $\dot{q}''_{w2} = h_{2w}\left(T_w^* - T_2\right)/k_2^*$. The corresponding wall temperatures are $T_{1w} = T_1 - \dot{q}''_{1w}/h_{1w}$ and $T_{2w} = T_2 + \dot{q}''_{w2}/h_{2w}$. The wall temperatures are important for estimation of the heat transfer regime between the walls and both fluids.

8.5.2 Benchmark for once through steam generator design with complex computer codes

Hassan and Morgan (1983) and Singhal et al. (1983) reported a once through steam generator test with counter-current flow. The geometry is presented in Fig. 8.13. The initial and the boundary conditions are given also by the authors. Measured are the fluid temperatures at both sides. The comparison between the computed and the measured temperatures is presented in Fig. 8.14(a) and (b) (at the boiling side the temperature of the wall wetting phase is plotted).

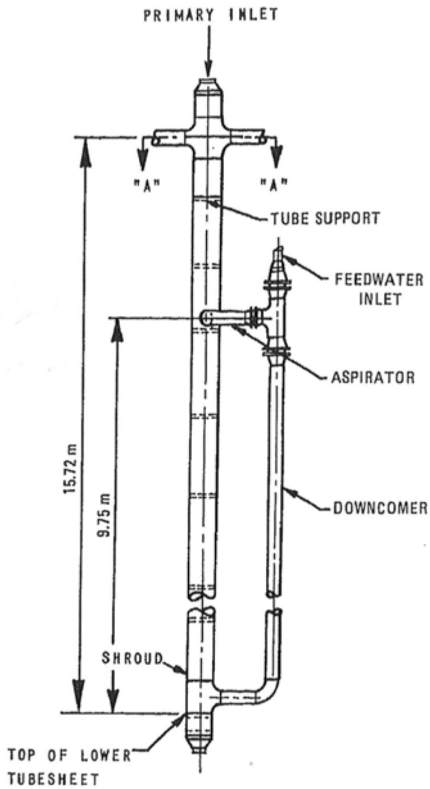

(a)

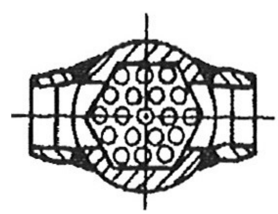

(b)

Fig. 8.13 Once through SG test section arrangement: (**a**) shroud with heat-exchanger pipes (left) and feed-water line (right); (**b**) section A-A, Hassan and Morgan (1983), Singhal et al. (1983)

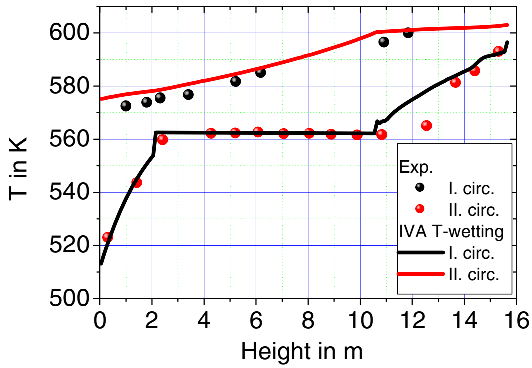

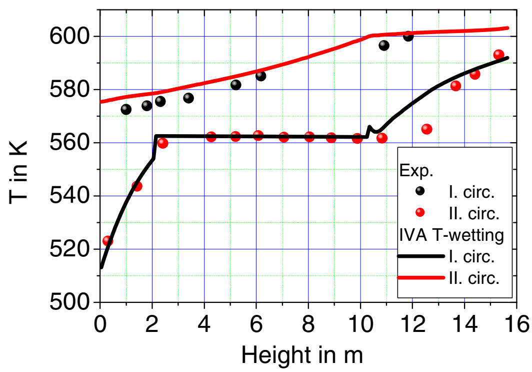

Fig. 8.14 Temperatures along the pipes for both sides of co-current heat exchangers: (a) CHF: Smolin et al. (1977), post CHF HTC transition boiling: Ramu and Weisman (1974); (b) CHF Lookup Table 2005: Groeneveld et al. (2005), Post CHF HTC transition boiling tubes: Groeneveld (1977)

We see that the section for heating the water up to the boiling point, the boiling section, and the superheating sections are well predicted.

8.5.3 Three-dimensional benchmarks – comparison with predictions of older computer codes

John et al. (2005) documented the geometry of a U-tube steam generator of the class 500 MWth and several computations with the computer codes THRUST and

ATHOS. The results obtained by repeating this analysis with the method presented in this monograph are presented in Figs. 8.15 to 8.19. The ATHOS and THRUST predictions differ for boundary conditions defining conditionally "15% from the nominal power" because the difference in the dome pressure (ATHOS and THRUST uses almost 60 bar) which is plausible.

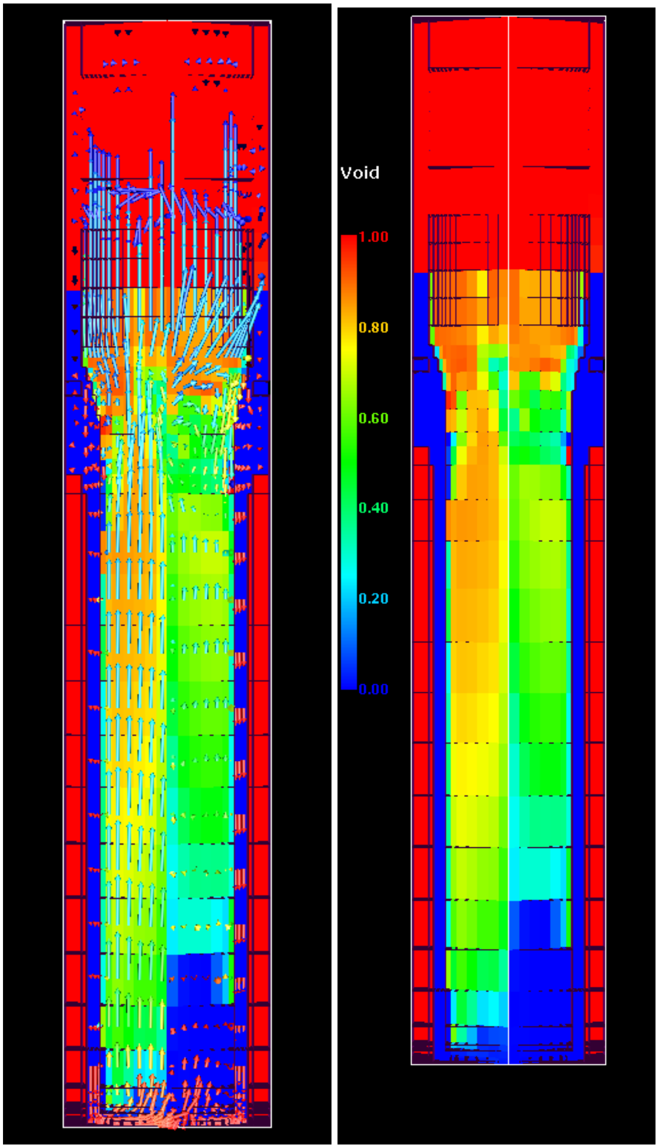

Fig. 8.15 Water velocity and void fraction for nominal case reported by John et al. (2005) computed with IVA computer code

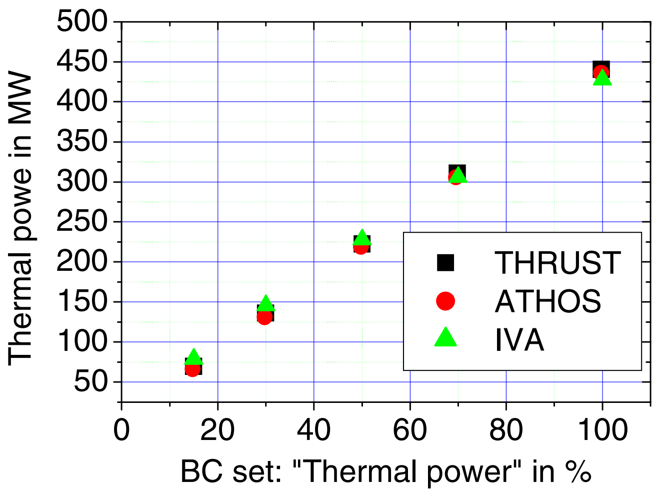

Fig. 8.16 Thermal power: IVA computed with the set of boundary conditions conditionally defined by 100, 75, 50, 30, 15%

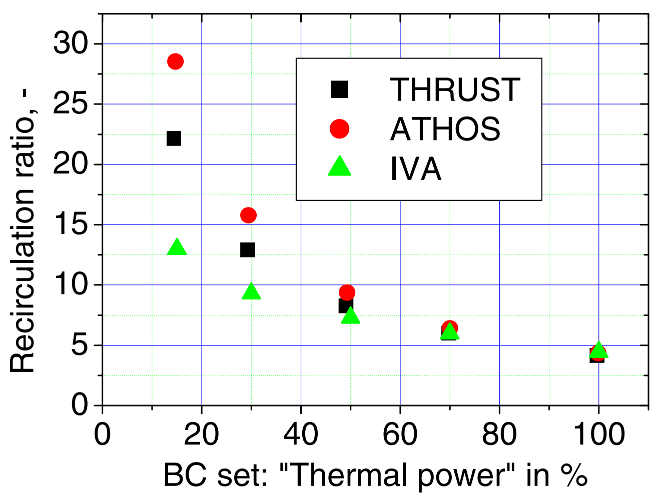

Fig. 8.17 Recirculation ratios: IVA computed with the set of boundary conditions conditionally defined by 100, 75, 50, 30, 15%

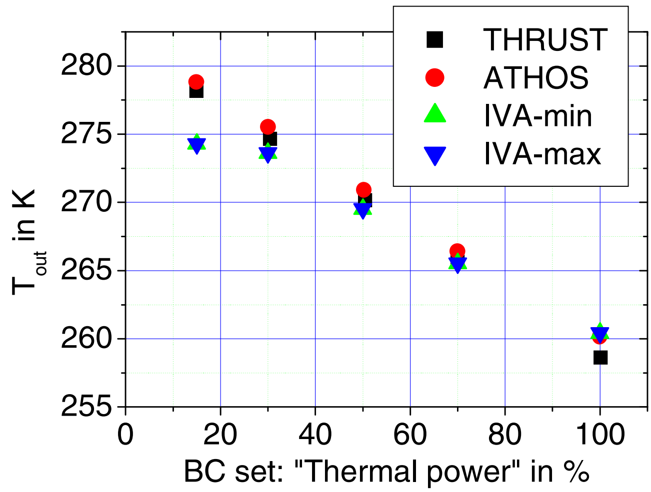

Fig. 8.18 Primary outlet temperatures: IVA computed with the set of boundary conditions conditionally defined by 100, 75, 50, 30, 15%

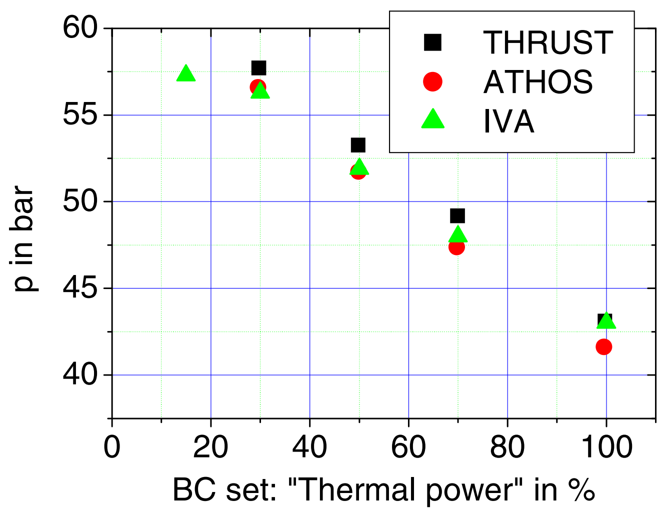

Fig. 8.19 Drum pressure: IVA computed with the set of boundary conditions conditionally defined by 100, 75, 50, 30, 15%

In general the differences are explained mainly in the very large difference in the physical modeling (ATHOS – drift flux model and thermal equilibrium (state of the art in the 1980s); IVA – modern three-fluid model and thermodynamic non-equilibrium). Other differences are in the modeling. The first difference is that the and THRUST models, as already mentioned, imposes a constant pressure at the exit of the cone section, whereas the IVA model imposes the pressure boundary condition at the exit nozzle which takes more processes into account, including the flow direction change through the dryer, acceleration pressure loss at the nozzle, etc. The second important difference is that ATHOS and THRUST impose a feed-water mass flow and a point model for mixing, whereas the IVA model uses natural mixing at the real positions, switching a numerical level controller. In general the modeling technology described in this monograph coded in the IVA computer code is powerful instrument for modern steam generation design.

8.6 Primary circuits of PWRs up to 1976

Pressurized water reactors compose almost 70% of the world's nuclear reactors. Usually they are built with three to six primary circuits. The most common technical solution up to 1976 was the four-loop system, as presented in Fig. 8.20.

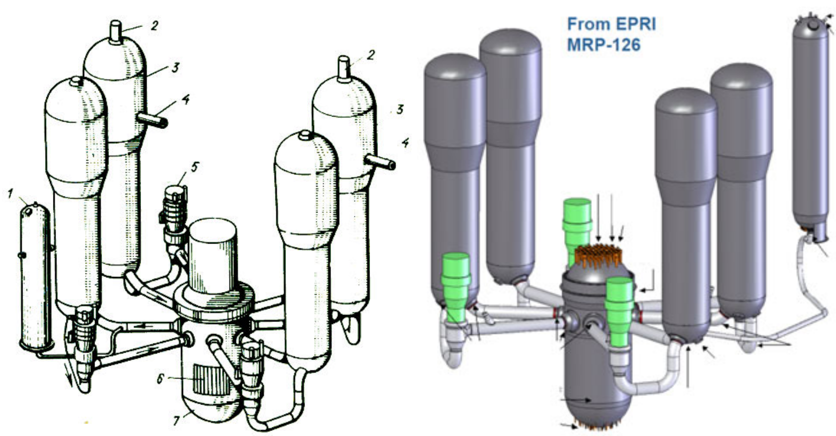

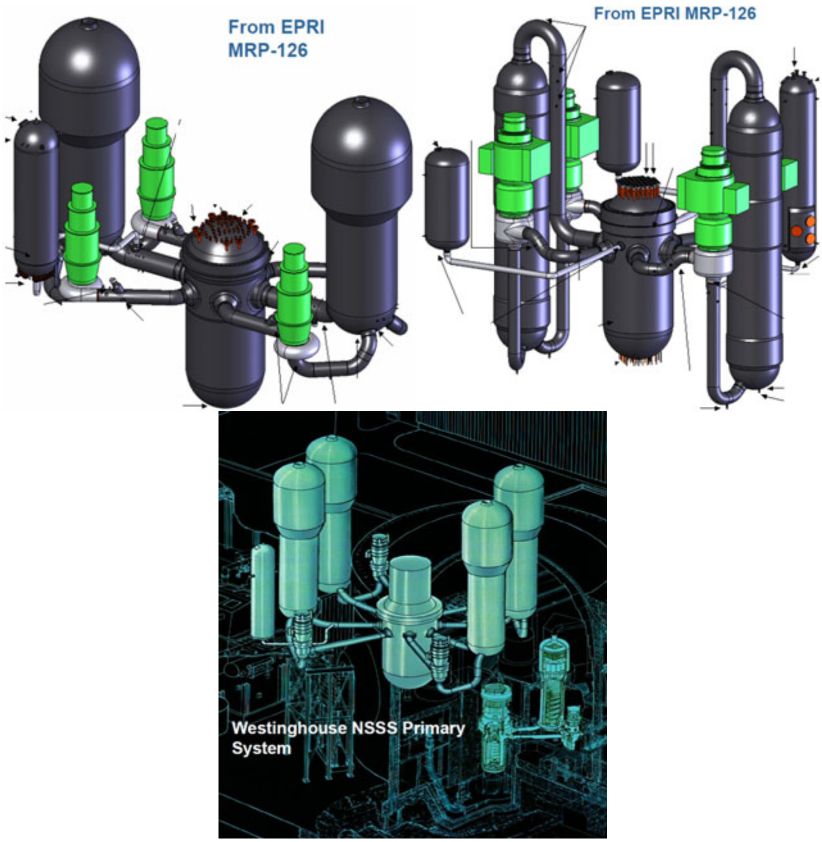

Fig. 8.20 Nuclear reactor coolant system of typical PWRs up to 1976: (a) 1. Pressurizer; 2. Steam nozzles; 3. Steam generators; 4. Feed-water line for the steam generators; 5. Main circulation pump; 6. Core; 7. Reactor pressure vessel, Rust and Weaver (1976), p.118; (b) Areva PWRs: 3 or 4 primary loops/recirculating SGs, 900–1500 MWe; Westinghouse PWRs: 2, 3, or 4 primary loops/recirculating SGs, 500–1200 MWe; (c) combustion-engine PWRs: 2 hot primary loops/recirculating SGs, 4 cold primary loops, 500–1300 MWe; (d) Babcock and Wilcox PWRs: 2 hot primary loops/once through SGs, 4 cold primary loops, 900 MWe, Clement (2009); (e) Westinghouse PWR, Maddox and Koontz (2000)

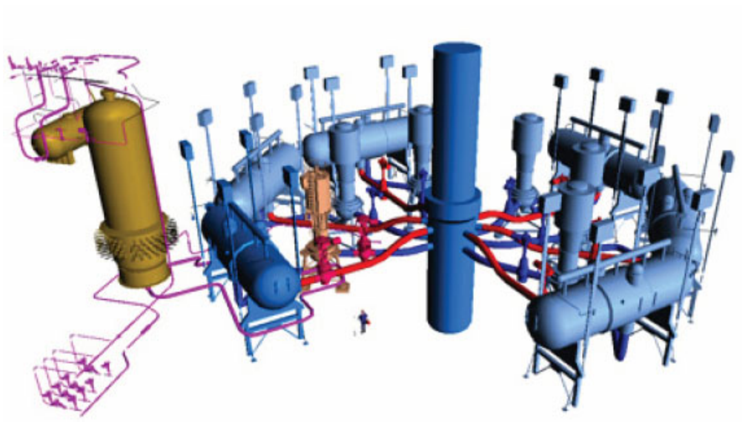

Fig. 8.21 Russian nuclear reactor coolant system of typical PWRs up to 1976 (VVER-440)

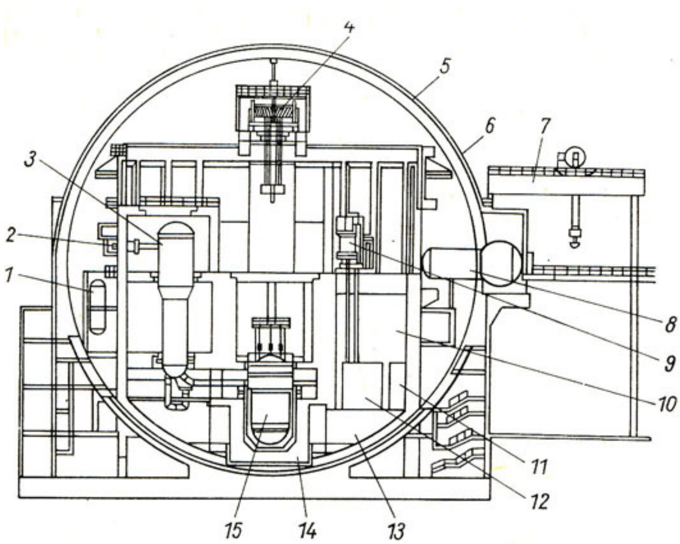

Fig. 8.22 Primary circuit layout of a Konvoi: 1. Hydro-accumulator; 2. Main steam line; 3. Steam generator; 4. Crane inside the containment; 5. external concrete containment shell; 6. Internal steel containment shell; 7. External crane; 8. Lock for material and equipment; 9. Loading machine; 10. In-containment refueling water storage; 11. Fresh-fuel container; 12. Place for deposition of the burned-fuel assemblies; 13. Drainage chamber; 14. Radiation protection; 15. Reactor pressure vessel, Margulowa (1976)

We see the components of the primary circuit: the nuclear reactor core, reactor pressure vessel containing the core, the four steam generators, the main circulation lines connected the vessel with the steam generators and four main circulation pumps forcing the coolant to circulate between the core and the primary side of

the steam generators. The steam generator can be vertical as shown in Fig. 8.20 and horizontal as shown in Fig. 8.21.

The primary circuit is placed inside a protection building called the containment. The design of the containments can be of different forms. One of the best solutions is presented in Fig. 8.22 where the primary circuit is placed inside a double-walled spherical containment. The internal wall protects the environment from any internal processes and the external wall protects the inside of the plant from any external events.

8.7 Primary circuits of modern PWRs

Except for the primary circuit of VVER-440, all other primary circuit designs presented in Fig. 8.23 are of modern reactors.

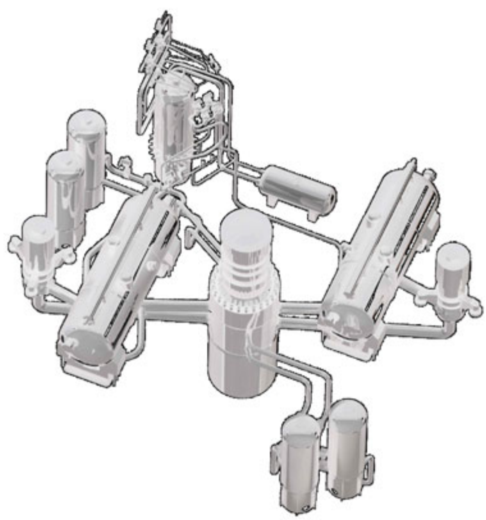

VVER-300 INR (2009)

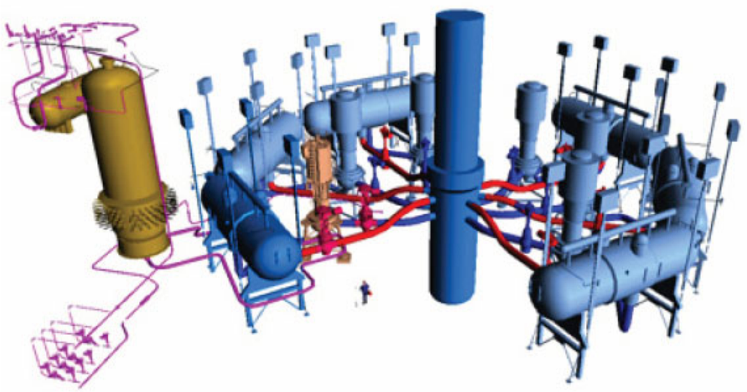

VVER-440 Böck (2009)

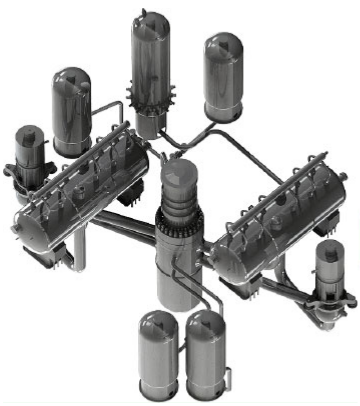

VVER-600 Ryjkov et al. (2009)

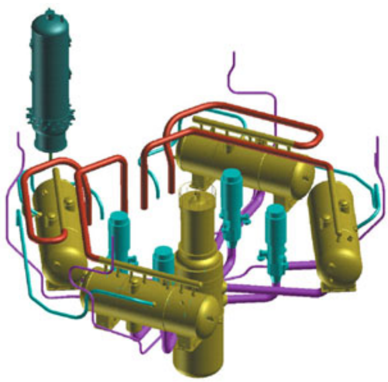

VVER-640 VVER-640 (2009)

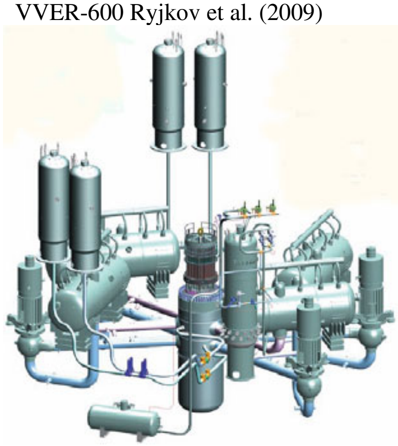

VVER-1000/466 OKB (2008)

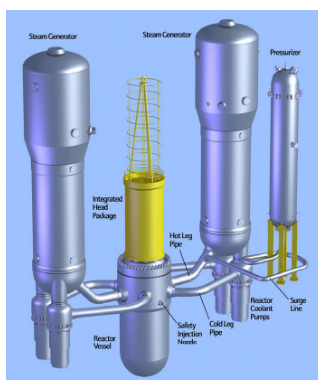

AP1000 Dagnall (2006)

ATMEA 1000 AREVA (2009)

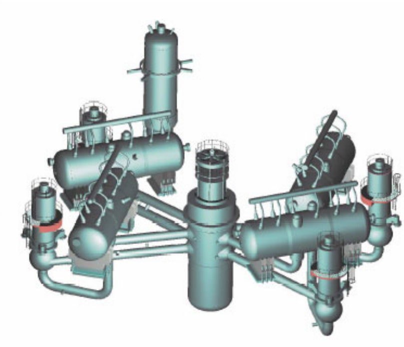

VVER-1200 Altshuller (2006)

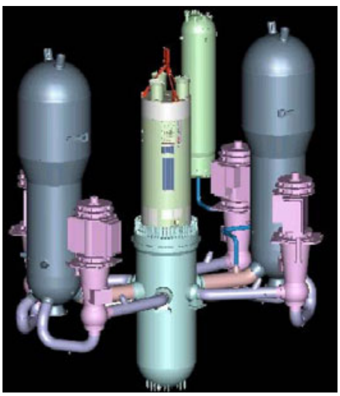

APR1400 Barré (2006)

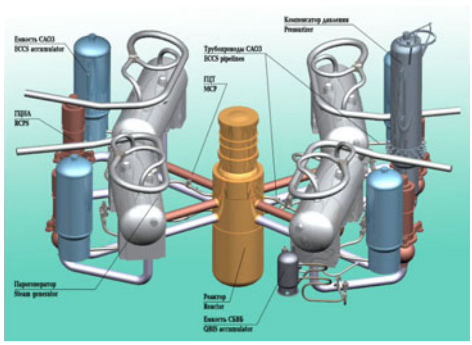

VVER-1500/1600 VVER-1500 (2009)

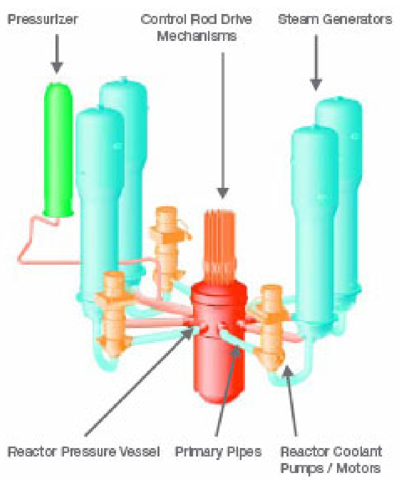

EPR 1600 EPR (1997)

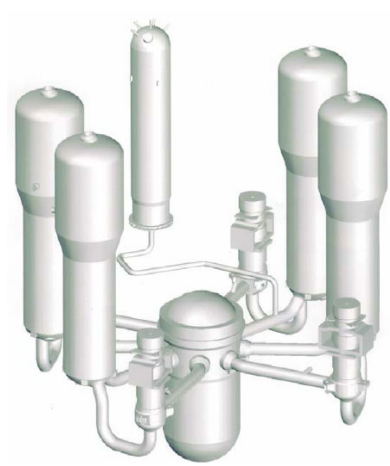

APWR 1700 Paulson (2008)

Fig. 8.23 Evolution of the primary circuit designs

Remarkably, the tendency to keep a 2–4 loop design with horizontal or vertical steam generators is retained.

Appendix 1 Some useful geometrical relations in preparing geometrical data for U-tube steam generator analysis

Hydraulic diameter: The hydraulic diameter is defined as four times the flow cross section divided by the wetted perimeter of the channel.

$$D_{hyd} = \frac{4F_{flow}}{\Pi_{wetted}}$$

So for a flow in a pipe we have

$$D_{hyd} = \frac{4F_{flow}}{\Pi_{wetted}} = \frac{4\pi D_i^2/4}{\pi D_i} = D_i ,$$

which is easy to remember. For cross section F penetrated perpendicularly by n_{pipes} with external diameter D_p the hydraulic diameter is

$$D_{hyd,p,\infty} = \frac{4F_{flow}}{\Pi_{wetted}} = 4\frac{F - n_{pipes}\pi D_p^2/4}{n_{pipes}\pi D_p} .$$

This definition which is valid for structured geometries is a limiting case of the more general definition

$$D_{hyd} = \frac{4V_{flow}}{F_{wetted}} ,$$

where we have instead of the flow cross section the flow volume of the computational cell V_{flow} and instead of the wetted perimeter the wetted surface F_{wetted} .

Heated diameter: The heated diameter is defined as four times the flow cross section divided by the heated perimeter of the channel.

$$D_{heated} = \frac{4F_{flow}}{\Pi_{heated}}$$

So for a flow in a heated pipe we have

$$D_{heated} = \frac{4F_{flow}}{\Pi_{heated}} = \frac{4\pi D_{p,i}^2/4}{\pi D_{p,i}} = D_{p,i}$$

which is easy to remember. For cross section F penetrated perpendicularly by n_{pipes} heat releasing pipes with external diameter D_p the heated diameter is

$$D_{heated} = \frac{4F_{flow}}{\Pi_{heated}} = 4\frac{F - n_{pipes}\pi D_p^2/4}{n_{pipes}\pi D_p}.$$

If there is additional not heated wall belonging to this cell the heated and the hydraulic diameters are different.

This definition valid for structured geometries is a limiting case of the more general definition

$$D_{heated} = \frac{4V_{flow}}{F_{heated}},$$

where we have instead of the flow cross section the flow volume of the computational cell V_{flow} and instead of the heated perimeter the heated surface F_{heated}.

Task 1: Given is an infinite bundle with triangular arrangement. The pipe diameter is D_p, see Fig. 8.11. The pitch is s. Compute the axial surface permeability $\gamma_{z,p}$ and the hydraulic diameter $D_{hyd,p}$.

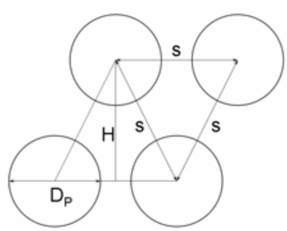

Fig. 8.24 Triangle pipe arrangement parameters

Solution 1: The high of the rhomb build by the centres of four neighbouring pipes is $H = \frac{\sqrt{3}}{2}s$, the surface of the rhomb $F_1 = s^2\sqrt{3}/2$. The permeability is

$$\gamma_{z,p,\infty} = \frac{F_1 - \pi D_p^2/4}{F_1} = 1 - \frac{\pi}{2\sqrt{3}}\left(\frac{D_p}{s}\right)^2 .$$

The hydraulic diameter is

$$D_{hyd,p,\infty} = \frac{4\left(F_1 - \pi D_p^2/4\right)}{\pi D_p} = \frac{\left(2\sqrt{3}s^2 - \pi D_p^2\right)}{\pi D_p} .$$

Task 2: Given an egg-grid cell with a large diagonal a and small diagonal s. The lengths of the sides are equal to each other, see Fig. 8.12. The thickness of the egg-grid inside the cell considered is b. Inside the grid there is a pipe with external diameter D_p. Compute the axial surface permeability $\gamma_{z,egg-grid,\infty}$ and the hydraulic diameter $D_{hyd,egg-grid,\infty}$.

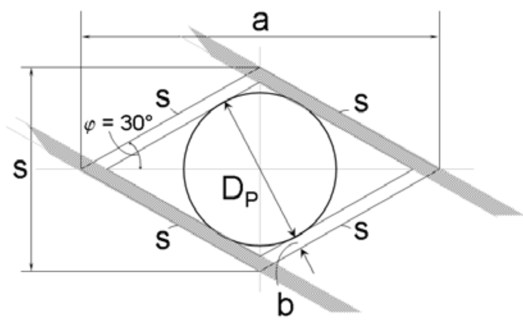

Fig. 8.25 Egg-spacer grid parameter

Solution 2: The surface of the elementary cell considered is $F_2 = \frac{1}{2}as$. The surface inside the egg-grid is $F_3 = F_2 - 2bs = s\left(\frac{1}{2}a - 2b\right)$. The axial permeability is then

$$\gamma_{z,egg-grid,\infty} = \frac{F_3 - \frac{\pi}{4}D_p^2}{F_2} = \frac{s\left(\frac{1}{2}a - 2b\right) - \frac{\pi}{4}D_p^2}{\frac{1}{2}as} = 1 - 4\frac{b}{a} - \frac{\pi}{2}\frac{D_p^2}{as} .$$

The corresponding hydraulic diameter is then

$$D_{hyd,egg-grid,\infty} = \frac{4\left(F_3 - \frac{\pi}{4}D_p^2\right)}{2s + \pi D_p} = \frac{4s\left(\frac{1}{2}a - 2b\right) - \pi D_p^2}{2s + \pi D_p}.$$

Task 3: Given a flow distribution plate cell. The pipe diameter is D_p. The hall diameter is $D_{FDP} > D_p$, see Fig. 8.13. The pitch is s. Compute the axial surface permeability $\gamma_{z,FDP,\infty}$ and the hydraulic diameter $D_{hyd,FDP,\infty}$.

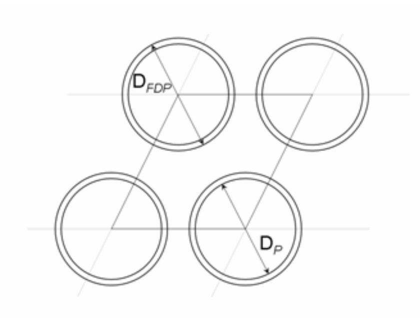

Fig. 26 Flow distribution plate in the regions outside the openings

Solution 3: The surface permeability is

$$\gamma_{z,FDP,\infty} = \frac{\frac{\pi}{4}\left(D_{FDP}^2 - D_p^2\right)}{F_1} = \frac{\pi}{2\sqrt{3}}\frac{\left(D_{FDP}^2 - D_p^2\right)}{s^2}.$$

The hydraulic diameter is then

$$D_{hyd,FDP,\infty} = \frac{4\frac{\pi}{4}\left(D_{FDP}^2 - D_p^2\right)}{\pi\left(D_{FDP} + D_p\right)} = D_{FDP} - D_p.$$

Task 4: Given are the tasks 1 to 3 with: s = 0.026 m, D_p = 0.019 m, a = 0.045032 m, b = 0.0029/2 m, D_{FDP} =0.0215 m. Compute $\gamma_{z,p,\infty}$, $D_{hyd,p,\infty}$, $\gamma_{z,egg-grid,\infty}$, $D_{hyd,egg-grid,\infty}$, $\gamma_{z,FDP,\infty}$, $D_{hyd,FDP,\infty}$.

Solution 4: The solution to 4 is $\gamma_{z,p,\infty} = 0.5157$, $D_{hyd,p,\infty} = 0.02023$ m, $\gamma_{z,egg-grid,\infty} = 0.3869$, $D_{hyd,egg-grid,\infty} = 0.0081$m, $\gamma_{z,FDP,\infty} = 0.1358$, $D_{hyd,FDP,\infty} = 0.0025$ m.

Task 5: Consider infinite rod bundle array with egg-grid having a thickness $L = \delta_{egg-grid}$ = 0.02 m. Compute the irreversible pressure loss coefficient with respect to the inlet cross section by taking into account also the friction coefficient for fully developed turbulent flow $\lambda = 0.02$ inside the grid channel.

Table 8.1 Irreversible friction pressure loss coefficient for abrupt cross section changes, Chisholm (1983)

1	Sudden contraction	$\xi = \dfrac{1}{(C_{vc}\sigma)^2} - 1 - \dfrac{2}{\sigma^2}\left(\dfrac{1}{C_{vc}} - 1\right)$
2	Thin plate	$\xi = \dfrac{1}{(C_{vc}\sigma)^2} - 1 - 2\left(\dfrac{1}{C_{vc}\sigma} - 1\right)$
3	Sudden enlargement	$\xi = -\dfrac{2}{\sigma}\left(1 - \dfrac{1}{\sigma}\right)$
4	Thick plate	$\xi = \dfrac{1}{(C_{vc}\sigma)^2} - 1 - \dfrac{2}{\sigma^2}\left(\dfrac{1}{C_{vc}} - 1\right) - 2\left(\dfrac{1}{\sigma} - 1\right)$
5	Globe valve	$\xi = 6$
6	Gate valve	$\xi = 0.17$
7	Contraction coefficient	$C_{vc} = \dfrac{1}{0.639(1-\sigma)^{1/2} + 1}$
8	Contraction ratio	σ = ratio downstream/upstream areas

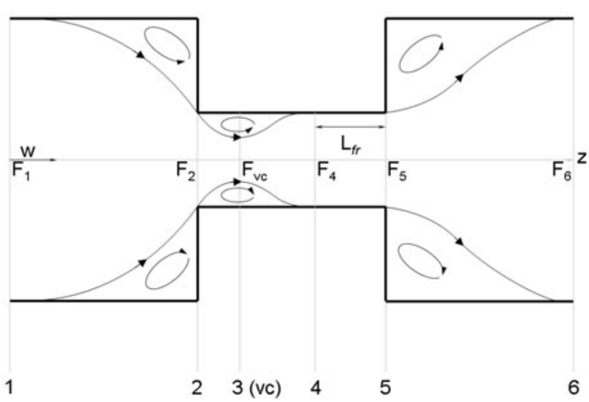

Fig. 27 Abrupt cross section changes in channel

Solution 5: Irreversible friction pressure loss coefficient for abrupt cross section changes (thick nozzle in a pipe) with respect to the inlet (or outlet) cross section with friction in accordance with Chisholm (1983) is given in Table 8.1. The contraction ratio is

$$\sigma = \frac{\gamma_{z,egg-grid,\infty}}{\gamma_{z,p,\infty}} = 0.75.$$

Selecting the thick plate solution No. 3 from Table 8.1 without a friction results in about 0.293. Taking the friction along the complete 6 cm length results in

$$\xi = \frac{1}{\left(C_{vc}\sigma\right)^2} - 1 - \frac{2}{\sigma^2}\left(\frac{1}{C_{vc}} - 1\right) - 2\left(\frac{1}{\sigma} - 1\right) + \lambda \frac{L}{D_{hy}} \frac{1}{\sigma^2}$$

which gives about 0.555. In the reality the flow recovering requires some length so that the friction is really depending on the remaining L_{fr}.

Task 6: Consider infinite rod bundle with FDP having a thickness $L = \delta_{FDP}$. Compute the irreversible pressure loss coefficient with respect to the inlet cross section by taking into account also the friction coefficient for turbulent flow $\lambda = 0.02$ inside the FDP channel.

Solution 6: The solution is like for task 5 with

$$\sigma = \frac{\gamma_{z,FDP,\infty}}{\gamma_{z,p,\infty}} = 0.2633$$

resulting in 12.15 neglecting the friction. Considering friction along 2 cm this value changes to 14.46.

Task 7: Usually the egg grids have a special design holding geometry at their two ends. The space in the central lane is used for this purpose which results in additional flow blockage. Therefore the following simple case holds. Given two circles with radiuses r_m and r_{m-1}, and the half of the lane thickness δ. Compute the blockage surface as given in Fig. 8.15.

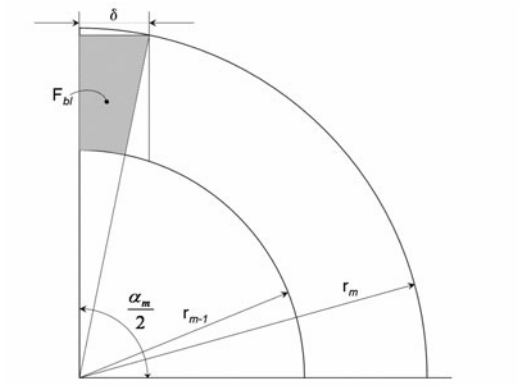

Fig. 8.28 Partial blockage in lane region

Solution 7: Text book solution gives

$$F_{bl} = \frac{1}{2}\left[r_m^2 \left(\pi - \alpha_m + \sin \alpha_m \right) - r_{m-1}^2 \left(\pi - \alpha_{m-1} + \sin \alpha_{m-1} \right) \right]$$

where

$$\alpha_m = \pi - 2 \text{ asin}\left(\delta / r_m \right).$$

References

Altshuller, A.: NPP-2006 with reactor VVER-1200/491 (2006), `http://www.reak.bme.hu/MTAEB/files/konferencia_20070308/tpresent/Atomstroyexport_03_SPbAEP_NPP-2006.pdf`

APR1400 Advanced power reactor 1400 (August 10, 2009a), `http://www.ats-fns.fi/archive/APR1400_Design_Characteristics.pdf`

APR1400, Plant Description, Korea Hydro & Nuclear Power (2009b), `http://www.khnp.co.kr/nutech/upload/APR1400%20Plant%20Description.doc`

AREVA, EPR, Areva brochure (2007)

AREVA, ATMEA1, Relible generation III+ solution world wide, AREVA brochure (2009)

ATMEA1 ATMEA1 – The mid-sized Generation III+ PWR you can rely on, Conference ETE – Siófok – Hungary (June 3, 2009)

Aubry, S., Cahouet, J., Nicolas, G., Niedergang, C.: A finite volume approach for 3D two phase flows in tube bundles the THYC code. In: Proceedings of the Fourth International Topical Meeting an Nuclear Reactor Thermal – Hydraulics, pp. 1247–1253 (1989)

B&W (2009), `http://www.babcock.com/bwc/nuclear_division/nuclear_broach.html`

Barré, B.: Futur du Nucléaire Nucléaire du Futur, Séminaire SLC (January 2006)

Bergunker, V.D.: 7th International Seminar on Horizontal Steam Generators, Podolsk, pp. 70–87 (2006)

Bibusmetals (2010), http://www.bibusmetals.ch

Böck, H.: WWER/ VVER (Soviet designed Pressurized Water Reactors Reactors), Lecture module 04, Vienna University of Technology /Austria (2009), http://www.ati.ac.at/fileadmin/files/research_areas/ssnm/nmkt/04_WWER_Overview.pdf

Bussy, B., Dague, G., Slama, G.: Starting up of new steam generator on N4 1450 MWe plants. In: Proc. 3th International Conference Steam Generators and Heat Exchanger, Toronto, Ontario, Canada (1998)

Carlucci, L.N., et al.: Thermal hydraulic analysis of the Westinghouse Model 51 steam Generator, EPRI NP2683 (1982)

Carson, W.R., Williams, H.K.: Methods of reducing carry-over and reducing pressure drop through steam separators, EPRI Final Report NP1607 (November 1980)

Clement R.: PWRs Systems and Operation (August 9, 2009), http://research.edf.com/fichiers/fckeditor/File/EDF%20RD/Printemps2008/18-11MAI/PWRs%20basics.pdf

Chisholm, D.: Two phase flow in pipelines and heat exchangers. George Godwin, London (1983)

Cumo, M., Naviglio, A. (eds.): Thermal hydraulic design of components for steam generation plants. CRC Press, Inc., Boca Raton (1991)

Cummins, E.: CSIS Nuclear Conference (June 26, 2008)

Dagnall, S.: AP1000 Technology for today's market practical options for a nuclear renaissance Institute of Physics, London (June 13, 2006)

Daehnerst, B.: The Westinghouse AP1000 reactor – and overview, Schweizerische Gesellschaft der Kernfachleute (March 6, 2007)

Doosan Heavy Industries & Construction, Creating values for the world nuclear power plants (2009)

Doosan: Steam Generator, Doosan Heavy Industries & Construction, DH0604 (2009b), http://www.doosanheavy.com/2/pdf/STEAM%20GENERATOR.pdf

Dragunov, Y., Ryzhov, S., Mokhov, V.: Development of WWER-1200 reactor plant for NPP of large series NPP-2006 (March 8, 2007)

Dueymes, E.: Wet steam flows in industrial large-diameter pipes: flow rate, moisture and pressure drop measurements. Int. J. Multiphase Flow 6(6), 901–909 (1989)

EPR, The European Pressurized Water Reactor called EPR, Nuclear Engineering International (October 1997)

EPR, Druckwasserreaktor 1600 MWe (EPR) Kernkraftwerk Olkiluoto 3, Finnland, Funktionsbeschreibung mit Poster, Broshure, Bestell-Nr.: ANP:G-46-V2-07-GER Printed in Germany 500115H WS 03076. K.-Nr. 309 (2009)

Fournier, R., Thibodeau, M., French, C.T.: Measurement of steam generator or reactor vessel moisture carryover using a non-radioactive tracer. In: Proc. of the 17th Int. Conf. on Nuclear Engineering, ICONE17, Brussels, Belgium, July 12-16 (2009)

Fortino, R.T., Oberjohn, W.J., Rice, J.G., Cornelius, D.K.: Thermal-Hydraulic Analyses of Once Through Steam Generators. EPRI NP-1431 (1980)

Gautier, D., Boissier, A.: Les pertes de charges et le transfert thermique cote gaz dans les échangeurs tubes lisses, a circulations orthogonales. Bulletin de la Direction des Etudes et Recherches d'EDF no. 2/3 (1971)

Gluhov, G.: Jadreni energiyni reactori, Tehnika, Sofia, Bulgaria (1979)

Green, S.J.: Thermal hydraulic and corrosion aspects of PWR steam generator problems. Heat Trans. Eng. 9, 1 (1988)

Green, S.J., Hetstroni, G.: PWR steam generators. Int. J. of Multiphase Flow 21(suppl.), 1–97 (1995)

Groeneveld, D.C.: Post-dryout heat transfer at reactor operating conditions. In: Nat. Topical Meet. Water Reactor Safety, Salt Lake City, Utah, American Nuclear Society, Conf. 730304, Rept. AECL-4513, March 26-28, Atomic Energy of Canada Ltd. (1977)

Groeneveld, D.C., et al.: The 1995 look-up table for critical heat flux in tubes. Nuclear Engineering and Design 163, 1–23 (1996)

Groeneveld, D.C., Shan, J.Q., Vasi, A.Z., Leung, L.K.H., Durmayaz, A., Yang, J., Cheng, S.C., Tanase, A.: The 2005 CHF look-up table. In: The 11th Int. Top. Meeting on Nuclear Thermal-Hydraulics (NURETH11), Avignon, France, October 2-6 (2005)

Gouirand, J.M.: CLOTAIRE Program – Thermal hydraulic test results in the straight part of the tube bundle. CEA/DTE/STRE/LGV/89/89/961 1 & 2 (1989)

Gouirand, J.M.: CLOTAIRE International Program – Final report – part 1 – Thermalhydraulic, CEA/DER/SCC/LTDE/91 /012 (1991)

Hassan, Y.A., Morgan, C.D.: Steady-state and transient prediction of a 19-tube once-through steam generator using RELAP5/MODI. Nucl. Tech. 60, 143–150 (1980)

Hassan, Y.A., Morgan, C.D.: Comparison of Lehigh 3 × 3 rod bundle post-CHF data with the predictions of RELAP5/MOD2. In: American Nuclear Society and Atomic Industrial Forum Joint Meeting, Washington, DC (1986)

IAEA-21, WWER-1000 reactor simulator, Workshop material. International Atomic Energy Agency, Training course series No. 21 (2003)

INR: Russian scientific centre "Kurtschatov Institute", Institute of Nuclear Reactors (2009), `http://www.inr.kiae.ru/ie.htm`

John, B., Dharne, S.P., Ghadge, S.G.: Evolution of 434 MWth steam generator to 540 MWth. In: The 11th International Topical Meeting on Nuclear Reactor Thermal-Hydraulics (NURETH-11) Paper: 332 Popes' Palace Conference Center, Avignon, France, October 2-6 (2005)

Keeton, L.W., Singhal, A.K., Irani, A.: A THOS3 code analysis of tube plugging effects an the thermal-hydraulic characteristics of a once-through steam generator. ASME 86-WA/NE-4 (1986)

Keeton, L.W., Singhal, A.K., Srikantiah, G.: ATHOS3: A computer program for thermal-hydraulic analysis of steam generators. vol. 1: Mathematical und Physical Models und Method of Solution; vol. 2: Programmer's Manual; Vol. 3: User's Manual. EPRI NP 4604-CCM, vol. 1-3, Revision 1 (1990)

Lee, J.Y., No, H.C.: Three-dimensional two-fluid code for U-tube steam generator thermal design analysis. In: Proc. 2nd International Topical Meetings an Nuclear Power Plant Thermal Hydraulics and Operations, Tokyo, Japan, 3-21 –3-27 (April 1986)

Lukasevich, B.I., Trunov, N.B., Likasevich, B.I., Dragunov Y.G., Dividenko, S.E.: Steam generators for VVER reactor facilities for nuclear power plants. IKTs Akademkniga, Moscow (2004)

Maddox, J., Koontz, F.: WATTS BAR Nuclear Power Plant Fundamentals Workshop (July 10, 2000)

Margulowa, T.C.: Kernkraftwerke, VEB Deutscher Verlag für Grundstoffindustrie, Leipzig (1976)

Miheev, M.A., Miheeva, I.M.: Osnovy teploperedachi, Energiya, Moskva (1973)

MNP Molybdenum and Nuclear Power – Part II (2009), `http://www.sprottmoly.com/pdf/NuclearMoly_2_.pdf`

Patankar, S.V., Spalding, D.B.: A calculation procedure for the transient and steady state behavior of shell-and-tube heat exchangers. Heat Exchanger Design and Theory Source Book, Scripta, Washington, DC (1976)

OKB, Reactor facilities for AES with VVER-1000 (2008), http://www.gidropress.podolsk.ru/publications/booklets/wwer1000_ru.pdf
Paulson, K.: Design Feature of US-APWR for Global Deployment, UAP-HF-07115 (July 21, 2008)
Pioro, I.L., Duffey, R.B.: Heat Transfer and Hydraulic Resistance at Supercritical Pressures in Power-Engineering Applications. Elsevier, Amsterdam (2007)
Prasser, H.-M.: Reactor technology: Complex 1 Design of Light Water Reactors, Lecture notes – an Internet publication, Eidgenössische Technische Hochschule Zürich, Swiss Federal Institute of Technology Zürich (2009)
Preuß, H.-J.: Entwiklingstendenzen und Zukunftsaufsichten. In: Oldekop, W. (ed.) Druckwasserreaktoren für Kernkraftwerke, ch. 14, p. 348. Verlag Karl Thiemig, München (1974)
Procaccia, H., et al.: Tests of types 51A and 51M steam generators at Bugey-4 and Tricastin-1 Nuclear Power Plants, EPRI NP-2689 (1982)
PWR, Pressurized water reactor, Siemens Brochure, Order No. A19100-U01-A148-V1-7600, Germany (March 1992)
Riboud, P.M., Brugeille, G.: Validation expérimentale du calcul thermo hydraulique bidimensionnel des échangeurs tubulaires. In: 22rad IAHR Congres, Lausanne, Switzerland, August 31-September 4 (1987)
RPWR, Russian pressurized water reactors VVER-440 & VVER-1000, internet publication (2009)
Rütz, J.: Messung der Frischdampffeuchte nach dem Drosselverfahren, Kernenergie, Jahrgang 16 Heft 1 S, 13–19 (1973)
Rust, J.H., Weaver, L.E.: Nuclear power safety. Pergamon Press, New York (1976)
Ryjkov, S.B., et al.: New projects for VVER power plants of medium size, International forum Atomexpo 2009, Moscow, CVK Expocenter (2009), (in Russian), Рыжов С.Б., Мохов В.А., Никитенко М.П., Четвериков А.Е., Щекин И.Г. (мая 26-28, 2009) Новые проекты реакторных установок ВВЭР средней мощности, Международный форум «АТОМЭКСПО 2009» г. Москва, ЦВК «Экспоцентр http://www.rosatom.ru/common/img/uploaded/for_PDF-news/Atomexpo/7_Chetverikov_Prezentatsiya_27.05.09_Atomekspo.ppt
SGSS Steam Generators and Steam Separators (2009), http://www.nucleartourist.com/systems/sg.htm
Singhal, A.K., Keeton, L.W., Srikantiah, G.: Thermal-Hydraulic Analysis of U-Tube and Once Through Steam Generators. In: AIChE Symposium Series 225, vol. 79, p. 331 (1983)
Singhal, A.K., Keeton, L.W., Przekwas, A.J., Weems, J.S.: ATHOS A Computer Program for Thermal Hydraulic Analysis of Steam Generators, vol. 4: Applications, EPRI NP-2698-CCM (1984)
Singhal, A.K., Srikantiah, G.: A review of thermal hydraulic analysis methodology for PWR steam generators and ATOS3 code applications. Prog. Nucl. Energy 25(1), 7–70 (1991)
Schwarz, T., Bouecke, R.: Utilization of the ATHOS code for split flow economizer and flow distribution plate calculations of steam generators. In: ASME Winter Annual Meeting Proc. HTD, vol. 51, pp. 57–69 (1985)
Smolin, V.N., Shpanskii, S.V., Esikov, V.I., Sedova, T.K.: Method of calculating burnout in tubular fuel rods when cooled by water and a water-steam mixture. Teploenergetika 24(12), 30–35 (1977)

Solomon, Y., Paine, J.P.N., Steininger, D.A., Williams, C.L.: Principles of steam generator degradation, Steam Generator Reference Book, ch. 5, EPRI (1985)

Ramu, K., Weisman, J.: A method for the correlation of transition boiling heat transfer data. In: Heat Transfer 1974, 5th Int. Heat Transfer Conf., Tokyo, vol. 4, pp. 160–164 (1974)

Ryjkov, S.B., et al.: New projects for VVER power plants of medium size, International forum Atomexpo 2009, Moscow, CVK Expocenter, in Russian: Рыжов С.Б., Мохов В.А., Никитенко М.П., Четвериков А.Е., Щекин И.Г. (мая 26-28, 2009) Новые проекты реакторных установок ВВЭР средней мощности, Международный форум «АТОМЭКСПО 2009» г. Москва, ЦВК «Экспоцентр (2009), http://www.rosatom.ru/common/img/uploaded/for_PDF-news/Atomexpo/7_Chetverikov_Prezentatsiya_27.05.09_Atomekspo.ppt

Trunov, N.B., Denisov, W., Kharchenko, S.A., Likasevich, B.I.: Taking account of operating experience when developing new designs for steam generators for nuclear power plants with VVER. Teploenergetica (1), 38–42 (2006)

Trunov, N.B., Likasevich, B.I., Veselov, D.O., Yu, G.: Steam generators – horizontal or vertical (which type should be used in nuclear power plants with VVER?). Atomic Energy 105(3), 165–174 (2008); translated from Atomnaya Energiya 105(3), 127–135 (September 2008)

US-APWR Nuclear Energy Systems Business Presentation Meeting Business Meeting Document 1, Nuclear Energy Systems Headquarters, Nuclear Headquarters Mitsubishi Heavy Industries (July 23, 2007d)

VVER-640, Reactor Plant with WWER-640 (V–407) for New Generation NPP Power Units (2009), http://www.gidropress.podolsk.ru/English/razrab_e.html

VVER-1500 Reactor Plant with WWER-1500 (V–448) for New Generation NPP Power Units (2009), http://www.gidropress.podolsk.ru/English/razrab_e.html

Wade, K.: Steam generation degradation and impact on continued operation of pressurized water reactors in the United States, Energy Information Administration. Electric Power Monthly, pp IX–XXI (August 1995)

Wang, S.S., Srikantiah, G.: Numerical modeling of the phase separation processes in BWR and PWR steam separators. In: AIChE Symp. Series, vol. 81, p. 245 (1985)